Safety and immunogenicity of booster vaccination and fractional dosing with Ad26.COV2.S or BNT162b2 in Ad26.COV2.S-vaccinated participants

Catherine Riou[1,2]*, Jinal N Bhiman[3,4]*, Yashica Ganga[5]*, Shobna Sawry[6]*, Frances Ayres[3,4], Richard Baguma[1], Sashkia R Balla[3,4], Ntombi Benede[1], Mallory Bernstein[5], Asiphe S Besethi[1], Sandile Cele[5], Carol Crowther[3,4], Mrinmayee Dhar[6], Sohair Geyer[1], Katherine Gill[7], Alba Grifoni[8], Tandile Hermanus[3,4], Haajira Kaldine[3,4], Roanne S Keeton[1], Prudence Kgagudi[3,4], Khadija Khan[5,9], Erica Lazarus[10], Jean Le Roux[6], Gila Lustig[11], Mashudu Madzivhandila[3], Siyabulela FJ Magugu[1], Zanele Makhado[3,4], Nelia P Manamela[3,4], Qiniso Mkhize[3,4], Paballo Mosala[1], Thopisang P Motlou[3,4], Hygon Mutavhatsindi[1], Nonkululeko B Mzindle[3], Anusha Nana[10], Rofhiwa Nesamari[1], Amkele Ngomti[1], Anathi A Nkayi[1], Thandeka P Nkosi[7], Millicent A Omondi[1], Ravindre Panchia[10], Faeezah Patel[6], Alessandro Sette[8,12], Upasna Singh[11], Strauss van Graan[3,4], Elizabeth M. Venter[3,4], Avril Walters[1], Thandeka Moyo-Gwete[3,4], Simone I. Richardson[3,4], Nigel Garrett[11,13], Helen Rees[6], Linda-Gail Bekker[7], Glenda Gray[14], Wendy A. Burgers[1,2]*, Alex Sigal[5,9,11]*, Penny L Moore[3,4,11]*, Lee Fairlie[6]*

Affiliations:
[1] Institute of Infectious Disease and Molecular Medicine, Division of Medical Virology, Department of Pathology, University of Cape Town, Observatory, South Africa
[2] Wellcome Centre for Infectious Diseases Research in Africa, University of Cape Town, Observatory, South Africa
[3] SA MRC Antibody Immunity Research Unit, School of Pathology, University of the Witwatersrand, Johannesburg, South Africa
[4] Center for HIV and STIs, National Institute for Communicable Diseases of the National Health Laboratory Services, Johannesburg, South Africa
[5] Africa Health Research Institute, Durban, South Africa.
[6] Wits RHI, Faculty of Health Sciences, University of the Witwatersrand, Johannesburg, South Africa
[7] The Desmond Tutu HIV Centre, University of Cape Town, Cape Town, South Africa
[8] Center for Vaccine Innovation, La Jolla Institute for Immunology, La Jolla, California, USA
[9] School of Laboratory Medicine and Medical Sciences, University of KwaZulu-Natal, Durban, South Africa.
[10] Perinatal HIV Research Unit, Faculty of Health Science, University of the Witwatersrand, Johannesburg, South Africa.
[11] Centre for the AIDS Programme of Research in South Africa, University of KwaZulu-Natal, Durban, South Africa.
[12] Department of Medicine, Division of Infectious Diseases and Global Public Health, University of California, San Diego (UCSD), La Jolla, California, USA
[13] Department of Public Health Medicine, School of Nursing and Public Health, University of KwaZulu-Natal, Durban, South Africa.
[14] South African Medical Research Council, Cape Town, South Africa

* These authors contributed equally
Corresponding Author: Lee Fairlie (LFairlie@wrhi.ac.za)

Abstract: 251 words, Full text: 11,773 words, Reference: 58.
Table: 1, Figures: 11, Supp tables: 2, Supp figure: 1.

ABSTRACT

Background. We report the safety and immunogenicity of fractional and full dose Ad26.COV2.S and BNT162b2 in an open label phase 2 trial of participants previously vaccinated with a single dose of Ad26.COV2.S, with 91.4% showing evidence of previous SARS-CoV-2 infection.

Methods. A total of 286 adults (with or without HIV) were enrolled >4 months after an Ad26.COV2.S prime and randomized 1:1:1:1 to receive either a full or half-dose booster of Ad26.COV2.S or BNT162b2 vaccine. B cell responses (binding, neutralization and antibody dependent cellular cytotoxicity-ADCC), and spike-specific T-cell responses were evaluated at baseline, 2, 12 and 24 weeks post-boost. Antibody and T-cell immunity targeting the Ad26 vector was also evaluated.

Results. No vaccine-associated serious adverse events were recorded. The full- and half-dose BNT162b2 boosted anti-SARS-CoV-2 binding antibody levels (3.9- and 4.5-fold, respectively) and neutralizing antibody levels (4.4- and 10-fold). Binding and neutralizing antibodies following half-dose Ad26.COV2.S were not significantly boosted. Full-dose Ad26.COV2.S did not boost binding antibodies but slightly enhanced neutralizing antibodies (2.1-fold). ADCC was marginally increased only after a full-dose BNT162b2. T-cell responses followed a similar pattern to neutralizing antibodies. Six months post-boost, antibody and T-cell responses had waned to baseline levels. While we detected strong anti-vector immunity, there was no correlation between anti-vector immunity in Ad26.COV2.S recipients and spike-specific neutralizing antibody or T-cell responses post-Ad26.COV2.S boosting.

Conclusion. In the context of hybrid immunity, boosting with heterologous full- or half-dose BNT162b2 mRNA vaccine demonstrated superior immunogenicity 2 weeks post-vaccination compared to homologous Ad26.COV2.S, though rapid waning occurred by 12 weeks post-boost.

Trial Registration: South African National Clinical Trial Registry (SANCR): DOH-27-012022-7841; **Funding:** South African Medical Research Council (SAMRC) and South African Department of Health (SA DoH).

Introduction

The development of vaccines against SARS-CoV-2 was unparalleled, with numerous platforms suited to rapid production dominating use in initial vaccination programs globally. This included adenovirus-vectored vaccines, such as the Janssen Ad26.COV2.S, replication-incompetent adenovirus 26 vectored SARS-CoV-2 spike protein vaccine. This vaccine is registered as a single dose, with subsequent boosters recommended. This was the first vaccine available nationally in South Africa, and health care workers, and later other essential workers, were offered this vaccine as part of the Sisonke trial [1]. The mRNA-based Pfizer BNT162b2 Comirnaty vaccine became available in South Africa subsequently as part of the national vaccine rollout.

The emergence of SARS-CoV-2 variants of concern (VOCs) including the Beta, Delta and Omicron variants reduced vaccine effectiveness against infection [2-6]. All vaccines based on the sequence of the SARS-CoV-2 ancestral spike, including the Janssen Ad26.COV2.S and the Pfizer Comirnaty BNT162b2 vaccines, elicited dramatically lower titers of neutralizing antibodies against the Omicron subvariants [4, 7-20]. Vaccines incorporating Omicron subvariant sequences [21] are not available in South Africa. However, the main driver of increased neutralizing capacity against Omicron variants is hybrid immunity, which is the combination of vaccine and infection elicited immunity. Population studies in SA showed seroprevalence levels in excess of 95% by the end of the Omicron BA.1 Wave [22]. However, given the waning of humoral and cellular immunity over time, COVID-19 vaccine boosting may be beneficial, especially in individuals at high risk for severe disease. The choice of booster, timing and dose remain largely dependent on regulatory and national considerations, including fiscal constraints and capacity of the health care system. Several studies have demonstrated a more robust humoral and cellular immune response with a heterologous boost compared to a homologous boost, in particular when boosting is with an mRNA vaccine [12, 15, 23]. A further consideration is that due to pressure on vaccine development, cost and equitable access, which are significantly impacted if multiple boosters

are needed, strategies such as fractional dosing should be considered. Fractional dosing has previously been used with other vaccines such as yellow fever [24].

South Africa is burdened by more HIV infections than any other country in the world, with approximately 8 million people living with HIV (PLWH) [25, 26]. PLWH, especially those with low CD4 T-cell counts, have moderately worse COVID-19 outcomes [27-35]. This is associated with lower and delayed neutralizing antibody titers in response to SARS-CoV-2 infection [19, 34, 36], more pronounced in PLWH with HIV viremia [19]. However, similar to results reported for the AstraZeneca ChAdOx and the Pfizer BNT162b2 vaccines [37-41], there was no observed difference between PLWH and HIV-negative individuals in neutralizing antibody titers against SARS-CoV-2 spike after Ad26.COV2.S vaccination [19, 36].

Vaccines which use a viral vector to deliver the immunogen may be inhibited by pre-existing immunity to the virus on which the vector is based [42, 43]. In addition to eliciting immunity to the vaccine target, vaccination with an adenovirus vectored vaccine has been shown to elicit neutralizing antibody and T-cell immunity to the vector itself [44-46]. This may reduce the ability of repeated doses of the vectored vaccine to infect cells or reduce vaccine vector-infected cell survival. The degree of elicited anti-vector immunity could therefore potentially determine the effectiveness of vectored immunization in a population with previous immunity to the virus on which the vector is based, or effectiveness if the vaccinees have been previously immunized with the same vector. However additional factors, including transgene persistence as well as local or systemic persistence may also impact the effectiveness of viral vectored vaccines.

In this study, we evaluated the immunogenicity and safety of diverse boost strategies after primary Ad26.COV2.S vaccination. We tested fractional and full dose heterologous and homologous booster Ad26.COV2.S and BNT162b2 vaccinations. We also determined the effects of HIV status, and degree of anti-adenovirus 26 vector immunity before and after boosting. We observed that heterologous boosting of Ad26.COV2.S with the BNT162b2 mRNA vaccine was the most effective regimen to transiently enhance humoral and T-cell immunity and HIV status did not have a substantial effect on the outcome. We show that

132 homologous boosting with Ad26.COV2.S occurred in the context of high anti-Ad26 vector
133 immunity. Although, Ad26.COV2.S gave a weak increase in antibody and cellular responses
134 against SARS-CoV-2 spike, we observed no correlation between vaccine response and anti-
135 Ad26 neutralizing antibody levels, as previously reported [47, 48].

Methods and Materials

Study Design and Participants. This study, **B**ooster **A**fter **Si**sonke **S**tudy (BaSiS), is an ongoing phase 2, randomized, open-label trial to evaluate the safety and immunogenicity of a booster vaccination in participants who received a single Ad26.COV2.S vaccine through the Sisonke phase 3B implementation study or via the South African National Department of Health COVID-19 vaccine rollout. Participants were healthy adults, who met study eligibility criteria and included participants with well-controlled comorbidities, except for HIV infection where there were no immunological or virological exclusions. Full eligibility criteria are provided in the protocol. We aimed to enrol at least one third of participants as PLWH and at least 10% >55 years of age. Participants were included if they had no SARS-CoV-2 infection at least 28 days prior to randomization. The study was conducted at four research sites in South Africa, two in Johannesburg, one in Durban and one in Cape Town.

Randomization. Participants were randomized 1:1:1:1 to one of four booster vaccinations including: Arm A: full-dose Ad26.COV2.S ($5x10^{10}$ vp/mL, 0.25 mL); Arm B: half-dose Ad26.COV2.S ($2.6x10^{10}$ vp/mL, 0.13 mL); Arm C: full-dose BNT162b2 Comirnaty vaccine (30mcg) and Arm D: half-dose BNT162b2 Comirnaty vaccine (15mcg). No masking was required since the study was open-label.

Procedures. Study visits took place at baseline (randomization), 2 weeks, 12 weeks and 24 weeks. At each visit, medical history, COVID-19 infection history (symptoms or positive test) and vaccination history (COVID-19 vaccine or other vaccination) was taken, followed by a targeted clinical examination when necessary. At the baseline visit, participants received a single booster vaccination, as per the randomization arm. Diary cards were issued and participants were trained to collect data up to 7 days post booster. Telephonic contact at day 7 was conducted to enquire about severity or ongoing nature of reactogenicity. Blood samples were drawn at each visit and included HIV testing at baseline (in all except those known to be PLWH), CD4 count and HIV viral load (in PLWH), full blood count (BL, W2 and additional visits in PLWH), D-dimers (BL and W2). A nasopharyngeal swab for SARS-CoV-2 PCR was

conducted at baseline. Interim visits were held for any safety concerns or if a participant had COVID-19 symptoms or a positive SARS-CoV-2 PCR or antigen test outside of the study.

Safety. Reactogenicity was collected and graded according to criteria included in Food and Drug Administration (FDA) "The Guidance for Industry: Toxicity Grading Scale for Healthy Adult and Adolescent Volunteers Enrolled in Preventive Vaccine Clinical Trials" [49]. All grade 3 reactogenicity events, SAEs, SUSARs and adverse drug reactions were reported. A Data Safety and Monitoring Committee was established to evaluate protocol-defined safety events and immunogenicity data.

Immunogenicity

Live virus neutralization assay

Live virus neutralization assay was performed as previously described in our previous work [4, 6, 18]. Briefly, ACE2-expressing H1299-E3 (CRL-5803, ATCC) cells were seeded at 4.5×10^5 cells per well and incubated for 18-20 h. After washing, the sub-confluent cell monolayer was inoculated with 500 µL universal transport medium diluted 1:1 with filtered growth medium. Cells were incubated for 1 h. Wells were then filled with 3 mL complete growth medium. After 4 days of infection (completion of passage 1), cells were trypsinized, centrifuged and resuspended in 4 mL growth medium. Then, all infected cells were added to Vero E6 cells (CRL-1586, ATCC). The coculture of ACE2-expressing H1299-E3 and Vero E6 cells was incubated for 4 days. The viral supernatant from this culture (passage 2 stock) was used for experiments.

H1299-E3 cells were plated at 30,000 cells/well 1 day pre-infection. Aliquots of cryo-preserved plasma samples were heat-inactivated and clarified by centrifugation. Virus stocks were used at approximately 50-100 focus-forming units per microwell and added to diluted plasma. Antibody–virus mixtures were incubated for 1 h at 37°C. Cells were infected with 100 µL of the virus–antibody mixtures for 1 h, then 100 µL of a RPMI 1640 (Sigma-Aldrich), 1.5% carboxymethylcellulose (Sigma-Aldrich) overlay was added without removing the inoculum. Cells were fixed 18 h post-infection. Foci were stained with a rabbit anti-spike monoclonal

antibody (0.5 µg/mL, BS-R2B12, GenScript) overnight at 4°C, washed and then incubated with a horseradish peroxidase (HRP) conjugated goat anti-rabbit antibody (1 µg/mL, Abcam ab205718) for 2 h. TrueBlue peroxidase substrate (SeraCare) was then added and incubated for 20 min. Plates were imaged in an ImmunoSpot Ultra-V S6-02-6140 Analyzer ELISPOT instrument with BioSpot Professional built-in image analysis (C.T.L). All statistics and fitting were performed using custom code in MATLAB v.2019b. Neutralization data were fit to: $Tx=1/1+(D/ID_{50})$. Tx is the number of foci normalized to the number of foci in the absence of plasma on the same plate at dilution D and ID_{50} is the plasma dilution giving 50% neutralization. $FRNT_{50} = 1/ID_{50}$. Values of $FRNT_{50}$ <1 are set to 1 (undiluted), the lowest measurable value. As, the most concentrated plasma dilution was 1:25, $FRNT_{50}$ <25 were extrapolated. To calculate confidence intervals, $FRNT_{50}$ or fold-change in $FRNT_{50}$ per participant was log-transformed and arithmetic mean plus and minus two standard deviations were calculated for the log transformed values. These were exponentiated to obtain the upper and lower 95% confidence intervals on the geometric mean $FRNT_{50}$ or the fold-change in $FRNT_{50}$ geometric means.

Sequences of outgrown ancestral SARS-CoV-2 and the Omicron BA.5 subvariant have been deposited in GISAID with accession EPI_ISL_602626.1 (ancestral, D614G) and EPI_ISL_12268493.2 (Omicron/BA.5).

SARS-CoV-2 spike and nucleocapsid enzyme-linked immunosorbent assay (ELISA)

For ELISA, Hexapro SARS-CoV-2 full spike protein with the D614G substitution were expressed in Human Embryonic Kidney (HEK) 293F suspension cells by transfecting the cells with the respective expression plasmid. After incubating for 6 days at 37°C, proteins were first purified using a nickel resin followed by size exclusion chromatography. Relevant fractions were collected and frozen at -80°C until use. Two µg/mL of D614G spike or nucleocapsid protein was used to coat 96-well, high-binding plates (Corning) and incubated overnight at 4°C. The plates were incubated in a blocking buffer consisting of 1x PBS, 5% skimmed milk powder, 0.05% Tween 20. Plasma samples were diluted to 1:100 starting dilution in a blocking

buffer and added to the plates. IgG secondary antibody (Merck) was diluted to 1:3000 in blocking buffer and added to the plates followed by TMB substrate (Thermofisher Scientific). Upon stopping the reaction with 1 M H2SO4, absorbance was measured at 450 nm. For spike ELISA, mAbs CR3022 was used as a positive control and Palivizumab was used as a negative control.

Lentiviral pseudovirus production and neutralization assay

Virus production and pseudovirus neutralization assays were done as previously described. Briefly, 293T/ACE2.MF cells modified to overexpress human ACE2 (provided by M. Farzan, Scripps Research) were cultured in DMEM (Gibco) containing 10% FBS and 3 µg/mL of puromycin at 37°C. Cell monolayers were disrupted at confluency by treatment with 0.25% trypsin in 1 mM EDTA (Gibco). The SARS-CoV-2, Wuhan-1 spike, cloned into pCDNA3.1 was mutated using the QuikChange Lightning Site-Directed Mutagenesis kit (Agilent Technologies) and NEBuilder HiFi DNA Assembly Master Mix (NEB) to include D614G (wild-type) or lineage defining mutations for Beta (L18F, D80A, D215G, 241-243del, K417N, E484K, N501Y, D614G and A701V), Delta (T19R, 156-157del, R158G, L452R, T478K, D614G, P681R and D950N), Omicron BA.1 (A67V, Δ69-70, T95I, G142D/Δ143-145, Δ211/L212I, ins214EPE, G339D, S371L, S373P, S375F, K417N, N440K, G446S, S477N, T478K, E484A, Q493R, G496S, Q498R, N501Y, Y505H, T547K, D614G, H655Y, N679K, P681H, N764K, D796Y, N856K, Q954H, N969K, L981F) and Omicron BA.4/5 (T19I, L24S, 25-27del, 69-70del,G142D, V213G, G339D, S371F, S373P, S375F, T376A, D405N, R408S, K417N,N440K, L452R, S477N, T478K, E484A,F486V, Q498R, N501Y, Y505H, D614G, H655Y, N679K, P681H, N764K, D796Y, Q954H, N969K). Pseudoviruses were produced by co-transfection in 293T/17 cells with a lentiviral backbone (HIV-1 pNL4.luc encoding the firefly luciferase gene) and either of the SARS-CoV-2 spike plasmids with PEIMAX (Polysciences). Culture supernatants were clarified of cells by a 0.45 µM filter and stored at -70°C. Plasma samples were heat-inactivated and clarified by centrifugation. Pseudovirus and serially diluted plasma/sera were incubated for 1 h at 37°C. Cells were added at 1×10^4 cells per well after 72 h of incubation at 37°C.

Luminescence was measured using PerkinElmer Life Sciences Model Victor X luminometer. Neutralization was measured as described by a reduction in luciferase gene expression after single-round infection of 293T/ACE2.MF cells with spike-pseudotyped viruses. Titers were calculated as the reciprocal plasma dilution (ID_{50}) causing 50% reduction of relative light units.

Antibody-dependent cellular cytotoxicity (ADCC) assay

The ability of plasma antibodies to cross-link FcγRIIIa (CD16) and spike expressing cells was measured as a proxy for ADCC as previously described. HEK293T cells were transfected with 5 µg of SARS-CoV-2 wild-type variant spike (D614G), Beta, Delta and Omicron BA.1 spike plasmids using PEI-MAX 40,000 (Polysciences) and incubated for 2 days at 37°C. Expression of spike was confirmed by binding of CR3022 and P2B-2F6 and their detection by anti-IgG APC (Biolegend) measured by flow cytometry. Subsequently, $1x10^5$ spike-transfected cells per well were incubated with heat inactivated plasma (1:100 final dilution) or control mAbs (final concentration of 100 µg/mL) in RPMI 1640 media supplemented with 10% FBS and 1% Pen/Strep (R10; Gibco) for 1 h at 37°C. Jurkat-Lucia™ NFAT-CD16 cells (Invivogen) ($2x10^5$ cells/well) were added and incubated for 24 h at 37°C. Twenty µl of supernatant was then transferred to a white 96-well plate with 50 µl of reconstituted QUANTI-Luc secreted luciferase and read immediately on a Victor 3 luminometer with 1s integration time. Cells were gated on singlets, live cells (determined by Live/dead™ Viability dye; Thermofisher Scientific), and those cells that were positive for IgG and spike specific monoclonal antibodies binding to their surface. Relative light units (RLU) of a no antibody control were subtracted as background. Palivizumab was used as a negative control, while CR3022 was used as a positive control, and P2B-2F6 to differentiate the Beta from the D614G variant. To induce the transgene, 1x cell stimulation cocktail (Thermofisher Scientific) and 2 µg/ml ionomycin in R10 was added as a positive control.

Measurement of antigen-specific T cells by flow cytometry

T-cell responses to SARS-CoV-2 spike or human adenovirus 26 (Ad26) hexon and penton were measured as previously described [3]. Briefly, cryopreserved PBMC were thawed, washed and rested in RPMI 1640 (Sigma-Aldrich) containing 10% heat-inactivated FBS (HyClone) for 4 h prior to stimulation. PBMC were seeded in a 96-well V-bottom plate at ~2x10^6 PBMC per well and stimulated with either a commercial ancestral SARS-CoV-2 spike (S) pool (1 µg/mL, Miltenyi Biotec) or a Ad26 peptide pool containing 293 peptides (15mers with 10-aa overlap) spanning the Ad26 hexon and penton proteins (1 µg/mL). All stimulations were performed in the presence of Brefeldin A (10 µg/mL, Sigma-Aldrich) and co-stimulatory antibodies against CD28 (clone 28.2) and CD49d (clone L25) (1 µg/mL each, BD Biosciences). As a negative control, PBMC were incubated with co-stimulatory antibodies, Brefeldin A and an equimolar amount of DMSO. After 16 h of stimulation, cells were washed, stained with LIVE/DEAD™ Fixable Near-IR Stain (Invitrogen) and subsequently surface stained with the following antibodies: CD14 APC-Cy7 (HCD14), CD19 APC-Cy7 (HIB19), CD4 BV785 (OKT4), CD8 FITC (RPA-T8), CD45RA BV570 (HI100) (Biolegend) and CD27 PE-Cy5 (1A4, Beckman Coulter). Cells were then fixed and permeabilized using a Cytofix/Cytoperm buffer (BD Biosciences) and stained with CD3 BV650 (OKT3), IFN-g BV711 (4S.B3), TNF-a PE-Cy7 (Mab11) and IL-2 PE/Dazzle™ 594 (MQ1-17H12) from Biolegend. Finally, cells were washed and fixed in CellFIX (BD Biosciences). Samples were acquired on a BD Fortessa flow cytometer and analyzed using FlowJo (v10.8.1, FlowJo LLC). Results are expressed as the frequency of total memory CD4+ or CD8+ T cells expressing IFN-g, TNF-a or IL-2. Due to high TNF-a backgrounds, cells producing TNF-a alone were excluded from the analysis. All data are presented after background subtraction.

Outcomes

The primary objectives of the study were to evaluate safety and reactogenicity and humoral and cellular immunogenicity to full and half dose homologous and heterologous booster vaccinations, at each study visit. Primary endpoint measures included measuring nucleocapsid binding antibody titers, neutralization titers and T-cell response magnitudes.

Safety was measured by participant self-report using diary cards and graded according to FDA standards [49]. The primary immunogenicity endpoint was defined as any study arm eliciting <75% of the highest geometric mean titre (GMT) response in the study. Together with the DSMB, the study team used this criteria to determine whether a subsequent booster should be offered to participants, and which booster if so. In this study, based on results, all participants except those who received the full dose BNT162b2 vaccination, were offered a full dose BNT162b2 booster in addition to that received according to their original randomisation.

Statistical Analysis

A two-tailed Wilcoxon signed-rank test or a Friedman test with Dunn's correction was used to assess statistical differences between paired samples. A Mann-Whitney test or a Kruskal-Wallis test with Dunn's corrections was used to compare multiple groups. Correlations were tested by a two-tailed non-parametric Spearman's rank test. In all cases, P values of less than or equal to 0.05 were considered significant.

Data Sharing

Protocol and data underlying the findings described in this manuscript may be obtained from the lead authors upon request.

Study Approval

This study has been approved by the South African Health Products Regulatory Authority (SAHPRA, number: 20210423) and all site-specific Human Research Ethics Committees (Wits: 211001B, UKZN: BREC/00003487/2021, UCT: 680/202). All participants provided written informed consent..

Results

Participants and follow up.

Between December 8, 2021, and July 27, 2022, 333 participants were screened and 289 randomized to 4 arms: Arm A: Full-dose Ad26.COV2.S ($5x10^{10}$ vp/mL, 74 participants); Arm B: half-dose Ad26.COV2.S ($2.6x10^{10}$ vp/mL, 69 participants); Arm C: Full-dose BNT162b2 (30mcg, 73 participants); and Arm D: half-dose BNT162b2 (15mcg, 73 participants) (**Table 1** and **Figure 1**). Participants were followed for 24 weeks, overall retention was 93.1% at 24 weeks (**Table 1**).

The majority of participants (53.6%, 155/289) were between 30 and 45 years old, with 36/189 (12.5%) 55 years and older, and 238/289 (82.4%) female. In the cohort, 116/289 (40.1%) were PLWH, 16 (13.8%) were considered viremic (VL >200cps/ml) and had a median CD4 count of 452 cells/mm^3 (IQR: 132-538), whereas participants who were virologically suppressed (VL <200cps/ml) had a median CD4 count of 708 cells/mm^3 (IQR: 558-922). At randomisation, subsequently referred to as baseline, 61/289 (21.1%) of participants had hypertension, 30/289 (10.4%) anaemia, and 174/289 (60.2%) were obese. Other comorbidities were less common (asthma and diabetes mellitus 4.2% each, arthritis 2.4% and tuberculosis 2.1% respectively).

Evidence of previous SARS-CoV-2 infection (positive nucleocapsid antibody detected by ELISA) was present in 91.4% (213/223) of participants tested at baseline indicating a high degree of hybrid immunity in the trial cohort. This was similar amongst the four vaccination arms, namely 91.2% (52/57), 87.9% (51/58), 93.2% (55/59) and 93.2% (55/59) for half-dose Ad26.COV2.S, full-dose Ad26.COV2.S, half-dose BNT162b2 and full-dose BNT162b2, respectively. These high levels of nucleocapsid positivity were sustained 2, 12 and 24 weeks after the booster dose, with greater than 80% nucleocapsid positivity at any given time point.

Participants received the booster vaccine at a median of 271 days (IQR: 255-296) after the Ad26.COV2.S prime. Nine breakthrough infections (BTI) were confirmed by SARS-CoV-2 PCR during the trial and all were mild infections that resolved within 4-12 days, 7/9 in the

Ad26.COV2.S arms. Three BTI occurred between W2 and W12, and the remainder between W12 and W24 (median: 17.1 weeks post boost).

Safety and reactogenicity of the booster vaccination regimens

Reactogenicity was measured through participant-completed diary cards, recording solicited local and systemic adverse reactions, as well as unsolicited adverse reactions through day-7 post booster, or longer if adverse events persisted. Overall, safety profiles were comparable between the four trial arms. Localised pain, headache, localised tenderness and weakness were reported with highest frequency, mostly of grade 1 and 2 severity. Grade 3 or 4 events included localised pain (2.0%), tenderness (1.7%), nausea (0.7%), diarrhoea (1.0%), headache (1.7%), weakness (2.8%), myalgia (1.0%), chills (0.7%), cough (0.3%), loss of smell (0.3%) and loss of taste (0.3%). Unsolicited AEs were uncommon, occurring in 8.7% of participants (**Figure 2**).

No events of thrombosis with thrombocytopenia syndrome (TTS) were reported; thrombocytopenia was reported in three participants, two had thrombocytopaenia at baseline. There were 14 serious AEs (SAEs) on study, non-related to study product, and no AEs of special interest (AESIs).

Antibody responses after booster vaccination

We evaluated spike binding antibody titers at baseline (BL) and week 2 (W2), week 12 (W12) and week 24 (W24) post-boost in the four vaccination arms using a trimeric spike ELISA for ancestral D614G virus. Relatively high spike binding antibody titers were detected in all groups at BL (geometric mean titer (GMT), $EC_{50:}$ >1000; **Figure 3A**). This is consistent with our observation that the majority of participants showed evidence of prior infection (**Table 1**). Spike antibody titers in the half- and full-dose Ad26.COV2.S arms were not significantly boosted by W2 (1.15 and 1.29 fold change in GMT, respectively), and did not change significantly up to W24. In contrast, half- and full-dose BNT162b2 arms demonstrated a significant increase in binding antibody titers at W2 (3.9 and 4.54 fold change, respectively), to

a GMT >4500 (**Figure 3A**). Spike binding antibodies in the BNT162b2 arms reduced to half that of W2 titers by W12, and had returned to BL levels by W24. These kinetics were reflected in a significantly higher fold-change between W2 and BL in the BNT162b2 arms compared to the Ad26.COV2.S arms (**Figure 3B**). Although waning had occurred by W12, EC_{50} titers in the BNT162b2 arms were still significantly higher than the Ad26.COV2.S arms (**Figure 3C**). While some differences between the arms persisted at W24, relatively high antibody titers, similar to those observed at BL and prior to a boost, were noted in all four arms, with GMT of 1016, 1140, 1563 and 1686 for half-dose Ad26.COV2.S, full-dose Ad26.COV2.S, half-dose BNT162b2 and full-dose BNT162b2, respectively.

Using a live virus neutralization assay, we evaluated neutralizing antibody titers to the ancestral D614G virus and Omicron BA.5, which was the most recent dominant sub-lineage at the time of W24 collection. At BL, neutralization activity against the D614G virus was similar between the arms (GMT $FRNT_{50}$ values of 546, 345, 393 and 334 for half-dose Ad26.COV2.S, full-dose Ad26.COV2.S, half-dose BNT162b2 and full-dose BNT162b2, respectively; **Figure 4A**). When measured at W2, half-dose Ad26.COV2.S did not boost BL neutralizing titers, while full-dose Ad26.COV2.S led to a 2.14-fold increase (**Figure 4B**). Both doses of BNT162b2 demonstrated a superior ability to boost neutralizing antibodies at W2 (8.5 to 10.2-fold compared to BL), with all but one participant increasing neutralizing titer (**Figure 4B**). As expected from its known immune evasion properties, $FRNT_{50}$ values for BA.5 neutralization were considerably lower than for ancestral virus (GMT of 84, 75, 84 and 63 for the four arms, respectively; **Figure 4C**). The kinetics mirrored those for D614G neutralization, with both doses of BNT162b2 demonstrating enhanced boosting of neutralizing antibodies compared to Ad26.COV2.S (**Figure 4D**). By week 24, neutralizing titers had waned significantly for the D614G virus, to a GMT of 732 and 840 for the BNT162b2 half- and full-doses, which was significantly higher than full-dose Ad26.COV2.S, with a GMT of 292 (**Figure 4E**). Neutralization of BA.5 was poor at W24 (GMT of 73-192), with no differences between the

groups. Five participants with documented BTI between W2 and W24 (**Figure 4A,C, red lines**) showed boosted neutralization activity, as expected.

In parallel, we assessed neutralizing antibody titers against an expanded panel of virus variants, namely D614G, Beta, Delta, Omicron BA.1 and BA.4/5 (which share identical spikes) using a lentiviral pseudovirus assay, limited to HIV-negative participants in the cohort. The data were consistent with our observations from the live virus assay, where significant boosting of neutralizing antibodies occurred at W2 against all variants for BNT162b2, but not for either the half- or full- dose Ad26.COV2.S (**Figure 5**). Titers against all variants declined from the W2 peak by W12, with a 2.4 to 5.7-fold drop, and levels remained constant to W24, with BNT162b2 arms trending to higher titers, regardless of the variant at W24.

Finally, we investigated antibody-dependent cellular cytotoxicity (ADCC) responses against the D614G, Beta, Delta and BA.1 spikes (**Figure 6A and 6B**) at BL and 2 weeks post-boost. As observed for the binding and neutralizing antibody responses, there was no increase in titers at W2 for either the half- or full-dose Ad26.COV2.S arms (median fold change 0.97 and 0.91, respectively), consistent with the fact that binding antibodies and ADCC potential are generally correlated. However, the half-dose BNT162b2 failed to trigger increased ADCC (median change 1.01), in contrast to the binding and neutralization results. For the full-dose BNT162b2 we observed marginally but nevertheless significantly higher ADCC titers against D614G, Beta and BA.1 spike at W2 compared to BL, but not to the same extent as binding or neutralizing responses.

T-cell responses before and after booster vaccination

We also measured SARS-CoV-2 spike-specific T-cell responses before and after homologous and heterologous vaccination with full or half-dose vaccines (n=214). Prior to boosting, spike-specific CD4+ responses were detected in most participants (>94.4%), with a frequency comparable between the four arms (**Figure 7A**). Two weeks after booster immunization, the

437 frequency of spike-specific CD4+ T cells was significantly increased in participants who
438 received BNT162b2 compared to BL (median: 0.23% vs 0.12% for half dose BNT162b2 and
439 0.25% vs 0.11% for full dose BNT162b2, respectively), while in participants boosted with
440 Ad26.COV2.S, the median frequency of SARS-CoV-2 spike-specific CD4+ T cells, while
441 statistically higher than BL, demonstrated only a marginal increase (0.12% vs 0.10% for half
442 dose and 0.15% vs 0.11% for full dose) (**Figure 7B**). The median fold change in CD4+
443 response between BL and W2 was significantly greater after a BNT162b2 booster (1.8 for half
444 dose and 1.98 for full dose) compared to an Ad26.COV2.S booster (1.1 for both half and full
445 dose; **Figure 7C**). Overall, ~80% of participants boosted with BNT162b2 (regardless of the
446 dose) had an increased spike-specific CD4+ T-cell response, while only 35.3% of participants
447 who received half dose Ad26.COV2.S and 43.4% in those receiving a full dose Ad26.COV2.S
448 booster expanded their CD4+ T-cell responses (**Figure 7D**). Spike-specific CD8+ T-cell
449 responses were less frequent than CD4+ responses, detected in only ~55% of the participants
450 at BL, and for those with a CD8+ response, the frequency of spike-specific CD8+ T cells was
451 comparable between the four groups at BL (**Figure 7E**). Two weeks after boosting, a
452 significant increase in the median CD8+ T-cell response was observed after a full-dose of
453 Ad26.COV2.S ($p = 0.002$) and both half- or full-dose of BNT162b2 ($p = 0.003$ and $p < 0.001$,
454 respectively; **Figure 7F**). Assessing only participants with a spike CD8+ response at both time
455 points, the median fold change at W2 post-boost was significantly higher after a BNT162b2
456 booster (1.91 for half-dose and 2.24 for full-dose) compared to an Ad26.COV2.S booster (1.22
457 for half-dose and 1.24 for full-dose; **Figure 7G**). However, it is important to note that individual
458 responses were highly variable within all groups, with spike-specific CD8+ responses
459 contracting, remaining negative or expanding. Overall, approximately half of participants
460 boosted with BNT162b2 displayed an increase in spike-specific CD8+ T-cell responses,
461 whereas an expansion of the CD8+ response was observed in only 1/3 of participants who
462 received a half-dose Ad26.COV2.S booster and ~40% in those receiving a full-dose
463 Ad26.COV2.S booster (**Figure 7H**).
464

The durability of T-cell responses was then assessed by measuring spike-specific T cells 24 weeks after the booster vaccination in a subset of participants (n=190). Pairwise comparison of spike-specific CD4+ T-cell frequencies at W24 relative to W2 demonstrated a significant contraction in the CD4+ response for all groups ($p < 0.001$ for both BNT162b2 boosters and half-dose Ad26.COV2.S and $p = 0.0047$ for full-dose Ad26.COV2.S), subsiding to BL levels (**Figure 8A**). Consequently, 24 weeks post-boosting, the magnitude of spike-specific CD4+ T cells was comparable in all trial arms (**Figure 8B**). In contrast, the median frequency of spike-specific CD8+ T cells appeared to increase between W2 and W24 in the Ad26.COV2.S group, although individual responses were highly variable, with some participants showing substantial waning or stable levels while others demonstrated gain of a CD8+ T-cell response that could be related to an undocumented BTI (**Figure 8C**). Overall, as for the CD4+ T-cell response, the frequency of spike-specific CD8+ T cells was similar across the four vaccine regimens when examined 24 weeks after booster vaccination (**Figure 8D**).

PLWH develop comparable antibody and T-cell responses after boosting

To determine whether HIV infection impacts vaccine booster responsiveness, participants were stratified by their HIV status. Prior to boosting, significantly lower titers of both binding and live virus neutralizing antibodies were found in PLWH who were viremic (viral load >200 HIV-1 mRNA copies/mL, n = 10) compared to virally suppressed individuals, who had similar antibody profiles to HIV-negative individuals (**Figure 9A-B**). Examination of baseline T-cell responses also revealed deficiencies, where significantly fewer viremic PLWH displayed spike-specific T-cell responses compared to aviremic and HIV-negative participants at BL (50% vs 100% and 97.6% for CD4+ and 10% vs 58.2% and 57.6% for CD8+; **Figure 9C-D**). Two weeks after booster vaccination, there was no difference in the degree of boosting (as measured by median fold-change between W2 and BL) for binding or neutralizing antibody titers between PLWH and HIV-negative participants for all vaccination groups (**Figure 9E-F**). For T-cell responses, however, the median fold change in CD4+ response in the full dose BNT162b2 group was significantly lower in PLWH compared to the HIV-negative participants

(1.52 vs 2.21, respectively, p = 0.037), with a trend towards lower fold-change in CD8+ spike T-cell responses in PLWH (p = 0.065; **Figure 9G-H**). Of note, a high proportion of viremic participants did not mount any CD4+ (4/10) or CD8+ T-cell responses (4/10) after any of the vaccine boosts, indicative of the impact of immunosuppression (**Supplementary Fig S1**).

At W24, comparable titers of binding and neutralizing antibodies were detected between PLWH and HIV-negative participants in all vaccination groups, and T-cell frequencies did not show any deficiencies in PLWH (**Figure 9I-L**). In fact, significantly higher frequencies of spike-specific CD4+ T cells were observed in PLWH in some vaccination groups (**Figure 9K**), possibly reflecting persistence of the higher baseline CD4+ T-cell responses observed in PLWH. Overall, these data suggest that some differences in the degree of boosting in PLWH, but by 24 weeks after revaccination, the frequencies of binding and neutralizing antibodies as well as spike-specific CD4+ and CD8+ T cells were comparable between HIV-negative participants and PLWH. This suggests that SARS-CoV-2 specific responses persist to a similar extent in those with well-controlled HIV infection compared to HIV-negative individuals. A proportion of viremic individuals, however, may be at risk of impaired T-cell responses and less durable antibody responses over the long term.

Anti-vector immunity is detectable but may not account for the limited ability of Ad26.COV2.S to boost spike-specific responses

We hypothesized that the muted capacity of Ad26.COV2.S to boost spike responses, compared to BNT162b2, may be due to anti-vector immunity, given that prior studies demonstrated that pre-existing Ad5 vector-specific nAbs and T cells have the capacity to limit responses to the transgene immunogen [44-46]. To measure anti-Ad26 neutralizing antibody activity, we established an Ad26 neutralization assay in which dilutions of plasma from vaccinees were mixed with the Ad26.COV2.S vaccine, and vector infection was measured by spike expression in the Ad26 vector infected cells (**Figure 10A-B**). To quantify Ad26-specific neutralizing activity before and after boosting, we titrated participant plasma to obtain the

plasma concentration needed to inhibit 50% of cellular infections with the Ad26 vector represented as ID_{50}, the reciprocal of this plasma dilution (**Figure 10C**). We tested 24 participants who had received full dose Ad26.COV2.S, and compared them to 24 participants who were boosted with BNT162b2, where no expansion of the vector-specific response would be expected. At BL, the majority of participants in both groups had Ad26-specific neutralizing antibody responses above the level of quantification (**Figure 10D**). Two weeks later, there was a significant increase in vector-specific ID_{50} in the Ad26.COV2.S boosted group ($p = 0.0006$), but no boosting in the group receiving BNT162b2 (median fold-change in nAb ID_{50} between W2 and BL: 1.83 for Ad26.COV2.S and 0.87 for BNT162b2; **Figure 10E**). To determine the level of neutralizing immunity against Ad26.COV2.S before primary Ad26.COV2.S vaccination, we investigated an independent cohort where participants were vaccinated with Ad26.COV2.S for the first time, with a subset accessing a second Ad26.COV2.S vaccine (**Supplementary Table 1**). The levels of anti-Ad26 neutralizing immunity prior to Ad26.COV2.S prime vaccination were below the level of quantification in all but one participant. Titers were significantly higher after an Ad26.COV2.S prime ($p <0.0001$; **Figure 10F**) but did not further increase after a boost, and were of similar magnitude to those in the BaSiS trial (**Figure 10F**). Finally, we investigated the association between Ad26-specific nAb titer at BL and the fold-change in spike neutralizing titer from W2 to BL, but found no correlation (**Figure 10G**).

To measure Ad26-specific T-cell responses, we stimulated PBMC with a pool of peptides spanning the viral hexon and penton proteins of Ad26 and characterized T-cell cytokine responses by flow cytometry. Ad26-specific T cells were readily detectable at BL and 2 weeks post-boosting (**Figure 11A**). We tested 44 participants who had received full-dose Ad26.COV2.S, and compared them to 20 participants who were boosted with BNT162b2, as a control group. At baseline, all participants in both groups had a CD4+ T-cell response to Ad26 (**Figure 11B**). Two weeks after Ad26.COV2.S booster vaccination, there was no overall increase in the Ad26-specific CD4+ response, which resembled the group who received the BNT162b2 booster. When comparing the fold-difference in the response from BL to W2, there

was a minor increase in the Ad26.COV2.S-boosted group (1.08 for Ad26.COV2.S and 0.91 for BNT162b2), reflecting a proportion of participants who had a marginal increase in the frequency of Ad26-specific CD4+ T cells (**Figure 11C**). We also investigated an independent unvaccinated healthcare worker cohort prior to Ad26.COV2.S vaccination (**Supplementary Table 2**); cross-sectional analysis indicated a significant, 3-fold higher magnitude of Ad26-specific CD4+ T-cell responses 4 weeks after vaccination ($p = 0.017$; **Figure 11D**), similar to what we observed for Ad26 nAb responses. Interestingly, 85% of participants had an existing adenovirus CD4+ response even before the priming dose, which is the likely result of conserved T-cell cross-reactivity due to infection with other adenoviral types.

Similarly, we characterized CD8+ T-cell responses specific for Ad26. These were detectable in 75% of participants at baseline, and unlike CD4+ responses, were boosted significantly ($p = 0.002$) by a second dose of Ad26.COV2.S, demonstrating an increase in response of 1.2 compared to 0.95 for the BNT162b2-boosted group (**Figure 11E** and **F**). CD8+ responses were more rare in the cohort not previously vaccinated with Ad26.COV2.S, detectable in only 35% of unvaccinated participants. These were significantly higher ($p = 0.005$) and detectable in 81.8% of individuals 4 weeks after initial Ad26.COV2.S vaccination, at a magnitude and range similar to the baseline responses in our trial (**Figure 11G**). Importantly, and consistent with Ad26-specific nAb responses, there was no association between the magnitude of Ad26-specific CD4+ or CD8+ T cells and spike-specific T-cell responses, either at BL or W2 (**Figure 11H**). Overall, anti-vector humoral and cellular immunity was abundantly detectable in our trial participants, but neither appeared to have a clear effect on dampening spike-specific responses.

Discussion

In this trial we evaluated the safety and immunogenicity of fractional and full doses of the Janssen adeno-vectored Ad26.COV2.S vaccine and the Pfizer BNT162b2 mRNA vaccine in an open label phase 2 trial of adults who had previously received a single dose of Ad26.COV2.S. The overwhelming majority of participants had detectable anti-nucleocapsid responses prior to receiving their boosts, indicating prior SARS-CoV-2 infection and boosting on the background of extensive hybrid immunity. We investigated safety and immunogenicity in both HIV-negative participants and PLWH, with the latter group generally well-controlled with VL suppression, and only 13.8% of PLWH being viremic (VL >200 cps/ml). Safety profiles in all four booster regimens were similar, with no regimen resulting in appreciable increased reactogenicity beyond localized responses at the injection site and mild, transient symptoms such as headache and weakness. Documented BTI, while few, mostly occurred in the Ad26.COV2.S boosted participants.

Heterologous boosting with the BNT162b2 mRNA vaccine was superior to homologous vaccination at early time points (2-12 weeks) by multiple humoral and cellular immune measures, including binding and neutralizing antibodies, and CD4+ T-cell responses to SARS-CoV-2 spike. This result is consistent with other studies showing better neutralizing antibody and T-cell responses after heterologous relative to homologous boosting of Ad26.COV2.S with an mRNA vaccine [23, 50]. Similar results were observed with mRNA vaccine heterologous boosting of the ChAdOx1 chimpanzee adeno-vectored vaccine [51, 52].

In contrast to the BNT162b2 vaccine, a homologous Ad26.COV2.S boost elicited limited, if any boosting of immune responses. Binding antibodies, neutralization, and T-cell responses increased 2-fold or less, and halving the dose resulted in no detectable booster activity. In contrast, boosting with BNT162b2 gave a 4- to 10-fold increase of antibody responses, with the exception of ADCC (discussed below), and 80% of trial participants had increased spike specific CD4+ T-cell responses. Unlike with Ad26.COV2.S, halving the dose of BNT162b2 did not strongly decrease the response to the booster in terms of either elicited binding antibodies, neutralizing antibodies, or CD4+ T-cell responses. Despite the strong boosting

effect of BNT162b2, waning of the binding and neutralizing antibody responses was pronounced by 12 weeks post-boost and by week 24, titers had declined close to the relatively high baseline titers. For ADCC, which generally correlates well with binding and neutralization, the absence of boosting by Ad26.COV2.S is expected, given the lack of boosting overall. However the marginal ADCC boosting observed only in the full-dose BNT162b2 arms (despite increased binding and neutralization) may be a consequence of class switching towards the IgG4 subclasses, which does not effectively mediate ADCC, as recently reported for repeated mRNA vaccination [53, 54].

The effects of HIV status on the neutralizing antibody and T-cell responses were moderate, and largely limited to reduced responses observed at baseline in PLWH with HIV viremia (despite the small size of this group). Both binding neutralizing antibody responses to ancestral SARS-CoV-2 were significantly lower in HIV viremic participants at baseline, while there was no difference between aviremic PLWH and HIV-negative participants. CD4+ T-cell responses showed a more marked difference with only 50% of viremic PLWH having detectable spike-specific CD4+ T cells, compared with 100% of aviremic PLWH and 97% of HIV-negative participants. For CD8+ T cells, the fraction of detectable spike-specific cells was 58% for both aviremic PLWH and HIV negative participants. In contrast, only 1 out of 10 HIV viremic participants had a detectable spike-specific CD8+ T-cell response. Interestingly, the median fraction of spike specific CD4+ T cells was significantly higher in aviremic PLWH than the HIV-uninfected participants, perhaps indicative of a different SARS-CoV-2 course of infection in PLWH [27] or interactions of SARS-CoV-2 immunity with HIV-mediated partial immune activation in HIV suppressed PLWH [55].

Post-boost, binding antibodies and neutralization were generally similar between PLWH and HIV negative participants. Even viremic PLWH showed increased binding and neutralizing antibody responses after BNT162b2 vaccination, and these were within the range seen in the other participants. These results are consistent with previous studies that PLWH have good antibody responses to vaccination [19, 38, 39, 56] with the exception of those with CD4+ T cell concentrations than 200 cells/mm^3 [34, 36, 37, 57, 58]. T-cell responses were more strongly

affected by HIV status: they were significantly lower for spike-specific CD4+ T cells in PLWH boosted with a full-dose of BNT162b2. We did not detect an increase in spike-specific CD8+ T-cell responses with full-dose BNT162b2, although the results did not reach statistical significance. The interpretation of the CD4+ T cell results is complicated by the higher median absolute fraction of spike-specific CD4+ T cells in PLWH post- BNT162b2 boost.

Although the Ad26.COV2.S is known to trigger lower responses than BNT162b2, the almost complete absence of boosting by this vaccine in our cohort was striking. We thus assessed whether this was caused by anti-vector immunity. Vaccination with adenovirus 5 vectored vaccines elicits both neutralizing antibody and T-cell immunity to the vector itself, decreasing the efficiency of cellular infection with the vaccine vector and attenuating the vaccine response [44-46]. Using the samples from this trial and supplementing with other cohorts where a pre-Ad26.COV2.S prime vaccination sample was available, we observed negligible Ad26.COV2.S neutralizing activity in vaccine-naïve donors. However, a single dose of Ad26.COV2.S strongly increases both neutralizing titers against Ad26.COV2.S and the fraction of Ad26-specific CD4+ and CD8+ T cells. Nevertheless, as with other studies of anti-Ad26.COV2.S neutralization, we could not find a clear association between the levels of anti-vector immunity, either neutralizing or T cell, and the degree of immune response post-Ad26.COV2.S boost, as previously reported [47, 48].

To conclude, we show that in the context of high levels of hybrid immunity, heterologous boosting with the BNT162b2 mRNA vaccine following a Ad26.COV2.S prime demonstrated superior immunogenicity and was safe and effective in both PLWH and HIV-negative participants, although there was a rapid waning of binding and neutralizing antibody responses. The Ad26.COV2.S homologous boost was also safe but showed highly attenuated immunogenicity relative to BNT162b2, both in antibody and T-cell immunity. While the Ad26.COV2.S vaccine elicited strong anti-vector immunity, we did not find clear evidence that this was the cause of attenuation.

Author contributions

Study design: LF, ASi, PLM, WAB, GG, L-GB, HR, SS, EL in collaboration with the sponsor (SAMRC). Data curation: JNB, TM-G, SS, NG, NN, EL. Experiment/investigation: RSK, RN, MAO, HM, RB, ANg, AW, SG, AAN, SFJM, ASB, NB, PM, SC, YG, KK, TM-G, ZM, EV, SvG, PK, QM, FA, SRB, TPM, TH, NPM, NBM, HK, MM, FP, JLR, SS, NG, NN, EL, RP, ANa. Methodology: WAB, CR, ASi, PLM, JNB, SIR, FP, SS. Data Analysis: WAB, CR, MPB, GL, ASi, PLM, JNB, SIR, LF, JLR, SS. Resource: AG, ASe. Project administration: WAB, ASi, PLM, JNB, CC, LF, FP, JLR, SS, NG, NN, TPN, MD, KMG. Writing (original draft): LF, PLM, ASi, WAB, CR, JNB, SS. Writing (review and editing): All authors reviewed and approved the final draft.

Acknowledgements and funding

We thank all the trial participants who contributed to this study. This study was funded by the South African Medical research Council (SAMRC), the Bill and Melinda Gates Foundation, through the Global Immunology and Immune Sequencing for Epidemic Response (GIISER) program (INV-030570) and the Wellcome Trust (226137/Z/22/Z). P.L.M is supported by the SAMRC (96833) and is an Department of Science and Innovation-National Research Foundation South African Research Chair (98341). A.Si. is supported by the Bill and Melinda Gates foundation (INV-046743) and the SAMRC (D2112300-01). W.A.B. is supported by the EDCTP2 program of the European Union's Horizon 2020 programme (TMA2016SF-1535-CaTCH-22) and the EU-Africa Concerted Action on SARS-CoV-2 Virus Variant and Immunological Surveillance (COVICIS), funded through the EU's Horizon Europe Research and Innovation Programme (101046041). C.R. is supported by the EDCTP2 program (TMA2017SF-1951-TB-SPEC). This project has also been funded in part by the National Institute of Allergy and Infectious Diseases, NIH, Department of Health and Human Services, under Contract No. 75N93021C00016 to A.G. and 75N93019C00065 to A.Se. The Wits RHI site received grant funding from Janssen to conduct the following clinical trials: Ensemble study (3UM1 AI068614-14SI), the Sisonke 1 study (96833), the Sherpa Study (96867) as well

as Pfizer for the Pfizer C4591015 study (C4591015), Horizon 1 (VAC31518COV2004) and Horizon 2 (VAC31518COV3006). For the purposes of open access, the authors have applied a CC-BY public copyright license to any author-accepted version.

Declaration of interest:

A.Se. is a consultant for AstraZeneca Pharmaceuticals, Calyptus Pharmaceuticals, Inc, Darwin Health, EmerVax, EUROIMMUN, F. Hoffman-La Roche Ltd, Fortress Biotech, Gilead Sciences, Granite bio., Gritstone Oncology, Guggenheim Securities, Moderna, Pfizer, RiverVest Venture Partners, and Turnstone Biologics. A.G. is a consultant for Pfizer. LJI has filed for patent protection for various aspects of T cell epitope and vaccine design work. All other authors declare no competing interests.

692 **Figure legends**

693

694 **Figure 1: Study design and CONSORT diagram. (A)** Study design. **(B)** CONSORT flow
695 diagram. BL: baseline, nAbs (Live): Live virus neutralization assay; nAbs (Pseudo):
696 pseudovirus neutralization assay. Binding Abs: Spike-specific IgG ELISA. ADCC: Antibody-
697 dependent cellular cytotoxicity assay. T-cell response: Spike-specific T-cell intracellular
698 cytokine staining assay.

699

700 **Figure 2: Recorded adverse events in each study arm.** Distribution of participants
701 experiencing adverse events (pain, headache, tenderness, weakness, nausea, diarrhea,
702 cough, myalgia, swelling, chills, loss of taste, redness, loss of smell or fever) recorded 1 week
703 post booster vaccination in each study arm.

704

705 **Figure 3: Spike-specific IgG responses over time in the immunogenicity sub-study**
706 **population. (A)** Longitudinal spike-specific IgG titer (EC_{50}) at baseline (BL), W2, W12 and
707 W24 after vaccine booster. The color-coded dots and bold lines represent the geometric mean
708 titer (GMT) at each time point. Recorded BTI between W2 and W24 are depicted with a red
709 line. Fold-change in the GMT is indicated at the bottom of each graph. Statistical comparisons
710 were performed using a Friedman test with Dunn's correction. **(B)** Fold change in spike-
711 specific IgG titer between W2 and BL in each study arm. Bars represent median fold change.
712 Statistical comparisons were performed using a Kruskal-Wallis test with Dunn's correction. **(C)**
713 Comparison of spike-specific IgG titer between study arms at W12 (left panel) and W24 (right
714 panel). Bars represent GMT. Statistical comparisons (in B and C) were performed using a
715 Kruskal-Wallis test with Dunn's correction.

716

717 **Figure 4: Live-virus neutralization activity against ancestral D614G and BA.5 SARS-**
718 **CoV-2 variant after booster vaccination.** Neutralizing titer ($FRNT_{50}$) against ancestral
719 D614G **(A&B)** and Omicron BA.5 **(C&D)** at BL and post-vaccine booster. **A&C** show titer at

BL, W2 and W24 post-boost for D614G **(A)** and BA.5 **(C)**. Fold-change of the GMT is indicated at the bottom of each graph. The color-coded dots and bold lines represent the GMT at each time point. Recorded BTI between W2 and W24 are depicted with red lines. Statistical comparisons were performed using a Friedman test with Dunn's correction. **B&D** show fold-change in neutralizing titer against D614G **(B)** and BA.5 **(D)** between BL and W2 in each study arm. Bars represent median fold-change. A Kruskal-Wallis test with Dunn's correction was used to compare different arm groups. **(E)** Comparison of the neutralizing titer ($FRNT_{50}$) against D614G (left panel) and BA.5 (right panel) between study arms at W24. Bars represent GMT. Statistical comparisons were performed using a Kruskal-Wallis test with Dunn's correction.

Figure 5: Pseudovirus neutralization activity against ancestral D614G, Beta, Delta, BA.1 and BA.4/5 SARS-CoV-2 variants after booster vaccination. Longitudinal neutralizing titer (ID_{50}) against ancestral D614G, Beta, Delta, Omicron BA.1 and BA.4/5 at BL, W2, W12 and W24 after vaccine booster. Bars represent medians. Bars represent GMT. Statistical comparisons were performed using a Kruskal-Wallis test with Dunn's corrections. Only HIV-negative participants were included in these analyses.

Figure 6: Antibody-dependent cellular cytotoxicity (ADCC) against ancestral (D614G), Beta, Delta and Omicron BA.1 SARS-CoV-2 variants. (A) ADCC (CD16 signalling) at BL and W2 in each study arm. Bars represent medians. The grey shaded area indicates an undetectable ADCC response. Statistical comparisons were performed using a Wilcoxon matched-pairs signed rank test. **(B)** Fold change in ADCC activity between W2 and BL in each study arm. Bars represent median fold change. Statistical comparisons were performed using a Kruskal-Wallis test with Dunn's corrections.

Figure 7: SARS-CoV-2 spike-specific T-cell responses before and 2 weeks after vaccine boosting. (A) Comparison of the frequency of spike-specific CD4+ T cells pre-boost in the

four study arms. The grey shaded area indicates undetectable response. **(B)** Frequency of spike-specific CD4+ T cells before (BL) and after vaccine boost (W2). **(C)** Fold change in the frequency of spike-specific CD4+ T cells between W2 and BL. **(D)** Overall profile of the evolution of the spike-specific CD4+ T-cell response between BL and W2. **(E)** Comparison of the frequency of spike-specific CD8+ T cells pre-boost in the four trial arms. **(F)** Frequency of spike-specific CD8+ T cells before (BL) and after vaccine boost (W2). **(G)** Fold change in the frequency of spike-specific CD8+ T cells between W2 and BL. **(H)** Overall profile of the evolution of the spike-specific CD8+ T-cell response between BL and W2. Bars represent medians. A two-tailed Wilcoxon signed-rank test was used to assess statistical differences between paired samples and a Kruskal-Wallis with Dunn's corrections was used to compare different groups.

Figure 8: Kinetics of SARS-CoV-2 spike-specific T-cell response after vaccination. (A) Longitudinal frequencies of spike-specific CD4+ T-cell responses induced by the four different booster vaccine regimens. **(B)** Comparison of the frequency of spike-specific CD4+ T cells between the four arms at W24 post-boost. **(C)** Longitudinal spike-specific CD8+ T-cell responses induced by the four booster vaccine regimens. **(D)** Comparison of the frequency of spike-specific CD8+ T cells between the four arms at W24 post-boost. The proportion of spike CD8+ responders is indicated at the top of the graph. The grey shaded area indicates undetectable response. The color-coded dots and bold lines in (A) and (C) represent the median at each time point. Recorded BTI between W2 and W24 are depicted with a red line. A Friedman test with Dunn's correction was used to assess statistical differences between paired samples and a Kruskal-Wallis with Dunn's corrections was used to compare different groups.

Figure 9: Humoral and cellular responses in study participants stratified by HIV status. (A to D) Spike-specific binding antibodies (A), live neutralization activity (B), spike-specific CD4+ response (C) and spike-specific CD8+ response (D) against ancestral (D614G) SARS-

776 CoV-2 in HIV-negative (HIV-), PLWH with a viral load <200 HIV mRNA copies/ml (HIV+ Avir)
777 and PLWH with a viral load >200 HIV mRNA copies/ml (HIV+ Vir) before vaccine booster (BL).
778 Bars represent GMT for A, B, I, J and medians for all other graphs. Statistical comparisons
779 were performed using a Kruskal-Wallis test with Dunn's corrections. The proportion of T-cell
780 responders is indicated on top of the graph. **(E to H)** Fold change in spike-specific binding
781 antibodies (E), live neutralization activity (F), spike-specific CD4+ response (G) and spike-
782 specific CD8+ response (H) between W2 and BL in each study arm, stratified by HIV status. **(I**
783 **to L)** Spike-specific binding antibodies (I), live neutralization activity (J), spike-specific CD4+
784 response (K) and spike-specific CD8+ response (L) against ancestral (D614G) SARS-CoV-2
785 at W24 after vaccine booster. Viremic PLWH are identified with a cross. Bars represent
786 medians. Statistical comparisons between PLWH and HIV-negative groups were performed
787 using a Mann-Whitney test.
788
789 **Figure 10: Ad26-specific neutralizing activity. (A)** Schematic representation of the Ad26-
790 specific neutralization assay. **(B)** Representative example of spike expression in
791 Ad26.COV2.S-infected H1299 cells measured by flow cytometry. **(C)** Representative example
792 of the inhibition of spike expression on Ad26.COV2.S-infected H1299 cells when
793 Ad26.COV2.S was pre-incubated with plasma (serial dilution) from a participant vaccinated
794 with one full dose of Ad26.COV2.S. **(D)** Ad26 neutralization activity (IC_{50}) pre- and W2 post full
795 dose-Ad26.COV2.S or a full-dose BNT162b2 booster. Statistical difference were assessed
796 using a Wilcoxon matched paired signed rank test. **(E)** Fold change in Ad26 neutralization
797 activity between W2 and BL in Ad26.COV2.S or BNT162b2 boosted participants. Bars
798 represent GMT for D and F and medians for E. Statistical differences were assessed using a
799 Wilcoxon matched paired signed rank test. **(F)** Comparison of Ad26 neutralization activity
800 (IC_{50}) in individuals who were vaccine naïve (n=14), received one full dose of Ad26.COV2.S
801 (n=14) or received two full doses of Ad26.COV2.S (n=6) from an independent cohort.
802 Statistical differences were assessed using a Kruskal-Wallis test with Dunn's correction. **(G)**
803 Relationship between the fold change in neutralizing titer against D614G SARS-CoV-2

between W2 and BL and Ad26 neutralization activity at BL. Correlation was tested by a two-tailed non-parametric Spearman's rank test.

Figure 11: Ad26-specific T-cell responses. (A) Representative example of IFN-g production in response to Ad26-specific peptide pool (hexon and penton) in one participant before (baseline) and 2 weeks after a full dose-Ad26.COV2.S booster. **(B & E)** Frequency of Ad26-specific CD4+ T cell (B) and CD8+ T cells (E) pre- and post a full dose-Ad26.COV2.S or a full-dose BNT162b2 booster. Statistical difference were assessed using a Wilcoxon matched paired signed rank test. **(C & F)** Fold change in the frequency of Ad26-specific CD4+ T cells (C) and CD8+ T cells (F) between W2 and BL in full-dose Ad26.COV2.S or full-dose BNT162b2 boosted participants. **(D & G)** Comparison of the frequency of Ad26-specific CD4+ T cells (D) and CD8+ T cells (G) in individuals who are vaccine naïve (n=20) or received one full dose of Ad26.COV2.S (n=11) from an independent cohort. The proportion of Ad26 T- cell responders is indicated at the top of each graph. Statistical differences were assessed using a Kruskal-Wallis test with Dunn's correction and a Chi-test to compare proportions. Bars represent medians. **(H)** Relationship between the frequency of spike-specific T-cell response at BL or W2 and the frequency of Ad26-specific T-cell responses at BL. Correlations were tested by a two-tailed non-parametric Spearman's rank test.

References

1. Bekker LG, Garrett N, Goga A, Fairall L, Reddy T, Yende-Zuma N, et al. Effectiveness of the Ad26.COV2.S vaccine in health-care workers in South Africa (the Sisonke study): results from a single-arm, open-label, phase 3B, implementation study. Lancet. 2022;399(10330):1141-53. doi: 10.1016/S0140-6736(22)00007-1. PubMed PMID: 35305740; PubMed Central PMCID: PMCPMC8930006.
2. Madhi SA, Baillie V, Cutland CL, Voysey M, Koen AL, Fairlie L, et al. Efficacy of the ChAdOx1 nCoV-19 Covid-19 Vaccine against the B.1.351 Variant. N Engl J Med. 2021;384(20):1885-98. Epub 20210316. doi: 10.1056/NEJMoa2102214. PubMed PMID: 33725432; PubMed Central PMCID: PMCPMC7993410.
3. Keeton R, Tincho MB, Ngomti A, Baguma R, Benede N, Suzuki A, et al. T cell responses to SARS-CoV-2 spike cross-recognize Omicron. Nature. 2022;603(7901):488-92. Epub 20220131. doi: 10.1038/s41586-022-04460-3. PubMed PMID: 35102311; PubMed Central PMCID: PMCPMC8930768.
4. Cele S, Jackson L, Khoury DS, Khan K, Moyo-Gwete T, Tegally H, et al. Omicron extensively but incompletely escapes Pfizer BNT162b2 neutralization. Nature. 2022;602(7898):654-6. Epub 20211223. doi: 10.1038/s41586-021-04387-1. PubMed PMID: 35016196; PubMed Central PMCID: PMCPMC8866126.
5. Wibmer CK, Ayres F, Hermanus T, Madzivhandila M, Kgagudi P, Oosthuysen B, et al. SARS-CoV-2 501Y.V2 escapes neutralization by South African COVID-19 donor plasma. Nat Med. 2021;27(4):622-5. Epub 20210302. doi: 10.1038/s41591-021-01285-x. PubMed PMID: 33654292.
6. Cele S, Gazy I, Jackson L, Hwa SH, Tegally H, Lustig G, et al. Escape of SARS-CoV-2 501Y.V2 from neutralization by convalescent plasma. Nature. 2021;593(7857):142-6. Epub 20210329. doi: 10.1038/s41586-021-03471-w. PubMed PMID: 33780970; PubMed Central PMCID: PMCPMC9867906.
7. Andrews N, Stowe J, Kirsebom F, Toffa S, Rickeard T, Gallagher E, et al. Covid-19 Vaccine Effectiveness against the Omicron (B.1.1.529) Variant. N Engl J Med. 2022;386(16):1532-46. Epub 20220302. doi: 10.1056/NEJMoa2119451. PubMed PMID: 35249272; PubMed Central PMCID: PMCPMC8908811.
8. Collie S, Champion J, Moultrie H, Bekker LG, Gray G. Effectiveness of BNT162b2 Vaccine against Omicron Variant in South Africa. N Engl J Med. 2022;386(5):494-6. Epub 20211229. doi: 10.1056/NEJMc2119270. PubMed PMID: 34965358; PubMed Central PMCID: PMCPMC8757569.
9. Dejnirattisai W, Huo J, Zhou D, Zahradnik J, Supasa P, Liu C, et al. SARS-CoV-2 Omicron-B.1.1.529 leads to widespread escape from neutralizing antibody responses. Cell. 2022;185(3):467-84 e15. Epub 20220104. doi: 10.1016/j.cell.2021.12.046. PubMed PMID: 35081335; PubMed Central PMCID: PMCPMC8723827.
10. Rossler A, Riepler L, Bante D, von Laer D, Kimpel J. SARS-CoV-2 Omicron Variant Neutralization in Serum from Vaccinated and Convalescent Persons. N Engl J Med. 2022;386(7):698-700. Epub 20220112. doi: 10.1056/NEJMc2119236. PubMed PMID: 35021005; PubMed Central PMCID: PMCPMC8781314.
11. Wilhelm A, Widera M, Grikscheit K, Toptan T, Schenk B, Pallas C, et al. Limited neutralisation of the SARS-CoV-2 Omicron subvariants BA.1 and BA.2 by convalescent and vaccine serum and monoclonal antibodies. EBioMedicine. 2022;82:104158. Epub 20220711. doi: 10.1016/j.ebiom.2022.104158. PubMed PMID: 35834885; PubMed Central PMCID: PMCPMC9271884.
12. Cheng SMS, Mok CKP, Leung YWY, Ng SS, Chan KCK, Ko FW, et al. Neutralizing antibodies against the SARS-CoV-2 Omicron variant BA.1 following homologous and heterologous CoronaVac or BNT162b2 vaccination. Nat Med. 2022;28(3):486-9. Epub 20220120. doi: 10.1038/s41591-022-01704-7. PubMed PMID: 35051989; PubMed Central PMCID: PMCPMC8940714.
13. Wang Q, Guo Y, Iketani S, Nair MS, Li Z, Mohri H, et al. Antibody evasion by SARS-CoV-2 Omicron subvariants BA.2.12.1, BA.4 and BA.5. Nature. 2022;608(7923):603-8. Epub

20220705. doi: 10.1038/s41586-022-05053-w. PubMed PMID: 35790190; PubMed Central PMCID: PMCPMC9385487.
14. McMenamin ME, Nealon J, Lin Y, Wong JY, Cheung JK, Lau EHY, et al. Vaccine effectiveness of one, two, and three doses of BNT162b2 and CoronaVac against COVID-19 in Hong Kong: a population-based observational study. Lancet Infect Dis. 2022;22(10):1435-43. Epub 20220715. doi: 10.1016/S1473-3099(22)00345-0. PubMed PMID: 35850128; PubMed Central PMCID: PMCPMC9286709.
15. Bowen JE, Addetia A, Dang HV, Stewart C, Brown JT, Sharkey WK, et al. Omicron spike function and neutralizing activity elicited by a comprehensive panel of vaccines. Science. 2022;377(6608):890-4. Epub 20220719. doi: 10.1126/science.abq0203. PubMed PMID: 35857529; PubMed Central PMCID: PMCPMC9348749.
16. Wang Y, Ma Y, Xu Y, Liu J, Li X, Chen Y, et al. Resistance of SARS-CoV-2 Omicron variant to convalescent and CoronaVac vaccine plasma. Emerg Microbes Infect. 2022;11(1):424-7. doi: 10.1080/22221751.2022.2027219. PubMed PMID: 35001836; PubMed Central PMCID: PMCPMC8803103.
17. Khan K, Karim F, Cele S, Reedoy K, San JE, Lustig G, et al. Omicron infection enhances Delta antibody immunity in vaccinated persons. Nature. 2022;607(7918):356-9. Epub 20220506. doi: 10.1038/s41586-022-04830-x. PubMed PMID: 35523247; PubMed Central PMCID: PMCPMC9279144.
18. Khan K, Karim F, Ganga Y, Bernstein M, Jule Z, Reedoy K, et al. Omicron BA.4/BA.5 escape neutralizing immunity elicited by BA.1 infection. Nat Commun. 2022;13(1):4686. Epub 20220810. doi: 10.1038/s41467-022-32396-9. PubMed PMID: 35948557; PubMed Central PMCID: PMCPMC9364294.
19. Khan K, Lustig G, Bernstein M, Archary D, Cele S, Karim F, et al. Immunogenicity of Severe Acute Respiratory Syndrome Coronavirus 2 (SARS-CoV-2) Infection and Ad26.CoV2.S Vaccination in People Living With Human Immunodeficiency Virus (HIV). Clin Infect Dis. 2022;75(1):e857-e64. doi: 10.1093/cid/ciab1008. PubMed PMID: 34893824; PubMed Central PMCID: PMCPMC8689810.
20. Richardson SI, Madzorera VS, Spencer H, Manamela NP, van der Mescht MA, Lambson BE, et al. SARS-CoV-2 Omicron triggers cross-reactive neutralization and Fc effector functions in previously vaccinated, but not unvaccinated, individuals. Cell Host Microbe. 2022;30(6):880-6 e4. Epub 20220325. doi: 10.1016/j.chom.2022.03.029. PubMed PMID: 35436444; PubMed Central PMCID: PMCPMC8947963.
21. Chalkias S, Harper C, Vrbicky K, Walsh SR, Essink B, Brosz A, et al. A Bivalent Omicron-Containing Booster Vaccine against Covid-19. N Engl J Med. 2022;387(14):1279-91. Epub 20220916. doi: 10.1056/NEJMoa2208343. PubMed PMID: 36112399; PubMed Central PMCID: PMCPMC9511634.
22. Madhi SA, Kwatra G, Myers JE, Jassat W, Dhar N, Mukendi CK, et al. Population Immunity and Covid-19 Severity with Omicron Variant in South Africa. N Engl J Med. 2022;386(14):1314-26. Epub 20220223. doi: 10.1056/NEJMoa2119658. PubMed PMID: 35196424; PubMed Central PMCID: PMCPMC8908853.
23. Sablerolles RSG, Rietdijk WJR, Goorhuis A, Postma DF, Visser LG, Geers D, et al. Immunogenicity and Reactogenicity of Vaccine Boosters after Ad26.COV2.S Priming. N Engl J Med. 2022;386(10):951-63. Epub 20220119. doi: 10.1056/NEJMoa2116747. PubMed PMID: 35045226; PubMed Central PMCID: PMCPMC8796791.
24. Vannice K, Wilder-Smith A, Hombach J. Fractional-Dose Yellow Fever Vaccination - Advancing the Evidence Base. N Engl J Med. 2018;379(7):603-5. Epub 20180711. doi: 10.1056/NEJMp1803433. PubMed PMID: 29995585.
25. Kharsany ABM, Cawood C, Khanyile D, Lewis L, Grobler A, Puren A, et al. Community-based HIV prevalence in KwaZulu-Natal, South Africa: results of a cross-sectional household survey. Lancet HIV. 2018;5(8):e427-e37. Epub 20180717. doi: 10.1016/S2352-3018(18)30104-8. PubMed PMID: 30021700; PubMed Central PMCID: PMCPMC7498647.
26. UNAIDS. HIV and AIDS Estimates South Africa. 2021. https://www.unaids.org/en/regionscountries/countries/southafrica2021.

27. Karim F, Gazy I, Cele S, Zungu Y, Krause R, Bernstein M, et al. HIV status alters disease severity and immune cell responses in Beta variant SARS-CoV-2 infection wave. Elife. 2021;10. Epub 20211005. doi: 10.7554/eLife.67397. PubMed PMID: 34608862; PubMed Central PMCID: PMCPMC8676326.
28. Geretti AM, Stockdale AJ, Kelly SH, Cevik M, Collins S, Waters L, et al. Outcomes of Coronavirus Disease 2019 (COVID-19) Related Hospitalization Among People With Human Immunodeficiency Virus (HIV) in the ISARIC World Health Organization (WHO) Clinical Characterization Protocol (UK): A Prospective Observational Study. Clin Infect Dis. 2021;73(7):e2095-e106. doi: 10.1093/cid/ciaa1605. PubMed PMID: 33095853; PubMed Central PMCID: PMCPMC7665382.
29. Ambrosioni J, Blanco JL, Reyes-Uruena JM, Davies MA, Sued O, Marcos MA, et al. Overview of SARS-CoV-2 infection in adults living with HIV. Lancet HIV. 2021;8(5):e294-e305. doi: 10.1016/S2352-3018(21)00070-9. PubMed PMID: 33915101; PubMed Central PMCID: PMCPMC8075775.
30. Western Cape Department of Health in collaboration with the National Institute for Communicable Diseases SA. Risk Factors for Coronavirus Disease 2019 (COVID-19) Death in a Population Cohort Study from the Western Cape Province, South Africa. Clin Infect Dis. 2021;73(7):e2005-e15. doi: 10.1093/cid/ciaa1198. PubMed PMID: 32860699; PubMed Central PMCID: PMCPMC7499501.
31. Davies MA. HIV and risk of COVID-19 death: a population cohort study from the Western Cape Province, South Africa. medRxiv. 2020. Epub 20200703. doi: 10.1101/2020.07.02.20145185. PubMed PMID: 32637972; PubMed Central PMCID: PMCPMC7340198.
32. Bhaskaran K, Rentsch CT, MacKenna B, Schultze A, Mehrkar A, Bates CJ, et al. HIV infection and COVID-19 death: a population-based cohort analysis of UK primary care data and linked national death registrations within the OpenSAFELY platform. Lancet HIV. 2021;8(1):e24-e32. Epub 20201211. doi: 10.1016/S2352-3018(20)30305-2. PubMed PMID: 33316211; PubMed Central PMCID: PMCPMC7773630.
33. Tesoriero JM, Swain CE, Pierce JL, Zamboni L, Wu M, Holtgrave DR, et al. COVID-19 Outcomes Among Persons Living With or Without Diagnosed HIV Infection in New York State. JAMA Netw Open. 2021;4(2):e2037069. Epub 20210201. doi: 10.1001/jamanetworkopen.2020.37069. PubMed PMID: 33533933; PubMed Central PMCID: PMCPMC7859843.
34. Spinelli MA, Lynch KL, Yun C, Glidden DV, Peluso MJ, Henrich TJ, et al. SARS-CoV-2 seroprevalence, and IgG concentration and pseudovirus neutralising antibody titres after infection, compared by HIV status: a matched case-control observational study. Lancet HIV. 2021;8(6):e334-e41. Epub 20210429. doi: 10.1016/S2352-3018(21)00072-2. PubMed PMID: 33933189; PubMed Central PMCID: PMCPMC8084354.
35. Walaza S, Tempia S, von Gottberg A, Wolter N, Bhiman JN, Buys A, et al. Risk Factors for Severe Coronavirus Disease 2019 Among Human Immunodeficiency Virus-Infected and -Uninfected Individuals in South Africa, April 2020-March 2022: Data From Sentinel Surveillance. Open Forum Infect Dis. 2022;9(12):ofac578. Epub 20221102. doi: 10.1093/ofid/ofac578. PubMed PMID: 36570970; PubMed Central PMCID: PMCPMC9772867.
36. Motsoeneng BM, Manamela NP, Kaldine H, Kgagudi P, Hermanus T, Ayres F, et al. Despite delayed kinetics, people living with HIV achieve equivalent antibody function after SARS-CoV-2 infection or vaccination. Front Immunol. 2023;14:1231276. Epub 20230803. doi: 10.3389/fimmu.2023.1231276. PubMed PMID: 37600825; PubMed Central PMCID: PMCPMC10435738.
37. Frater J, Ewer KJ, Ogbe A, Pace M, Adele S, Adland E, et al. Safety and immunogenicity of the ChAdOx1 nCoV-19 (AZD1222) vaccine against SARS-CoV-2 in HIV infection: a single-arm substudy of a phase 2/3 clinical trial. Lancet HIV. 2021;8(8):e474-e85. Epub 20210618. doi: 10.1016/S2352-3018(21)00103-X. PubMed PMID: 34153264; PubMed Central PMCID: PMCPMC8213361.

38. Levy I, Wieder-Finesod A, Litchevsky V, Biber A, Indenbaum V, Olmer L, et al. Immunogenicity and safety of the BNT162b2 mRNA COVID-19 vaccine in people living with HIV-1. Clin Microbiol Infect. 2021;27(12):1851-5. Epub 20210824. doi: 10.1016/j.cmi.2021.07.031. PubMed PMID: 34438069; PubMed Central PMCID: PMCPMC8382485.
39. Woldemeskel BA, Karaba AH, Garliss CC, Beck EJ, Wang KH, Laeyendecker O, et al. The BNT162b2 mRNA Vaccine Elicits Robust Humoral and Cellular Immune Responses in People Living With Human Immunodeficiency Virus (HIV). Clin Infect Dis. 2022;74(7):1268-70. doi: 10.1093/cid/ciab648. PubMed PMID: 34293114; PubMed Central PMCID: PMCPMC8406881.
40. Ruddy JA, Boyarsky BJ, Bailey JR, Karaba AH, Garonzik-Wang JM, Segev DL, et al. Safety and antibody response to two-dose SARS-CoV-2 messenger RNA vaccination in persons with HIV. AIDS. 2021;35(14):2399-401. doi: 10.1097/QAD.0000000000003017. PubMed PMID: 34261097; PubMed Central PMCID: PMCPMC10323870.
41. Brumme ZL, Mwimanzi F, Lapointe HR, Cheung PK, Sang Y, Duncan MC, et al. Humoral immune responses to COVID-19 vaccination in people living with HIV receiving suppressive antiretroviral therapy. NPJ Vaccines. 2022;7(1):28. Epub 20220228. doi: 10.1038/s41541-022-00452-6. PubMed PMID: 35228535; PubMed Central PMCID: PMCPMC8885829.
42. Saxena M, Van TTH, Baird FJ, Coloe PJ, Smooker PM. Pre-existing immunity against vaccine vectors--friend or foe? Microbiology (Reading). 2013;159(Pt 1):1-11. Epub 20121122. doi: 10.1099/mic.0.049601-0. PubMed PMID: 23175507; PubMed Central PMCID: PMCPMC3542731.
43. Ahi YS, Bangari DS, Mittal SK. Adenoviral vector immunity: its implications and circumvention strategies. Curr Gene Ther. 2011;11(4):307-20. doi: 10.2174/156652311796150372. PubMed PMID: 21453277; PubMed Central PMCID: PMCPMC4009923.
44. Casimiro DR, Chen L, Fu TM, Evans RK, Caulfield MJ, Davies ME, et al. Comparative immunogenicity in rhesus monkeys of DNA plasmid, recombinant vaccinia virus, and replication-defective adenovirus vectors expressing a human immunodeficiency virus type 1 gag gene. J Virol. 2003;77(11):6305-13. doi: 10.1128/jvi.77.11.6305-6313.2003. PubMed PMID: 12743287; PubMed Central PMCID: PMCPMC154996.
45. Barouch DH, Pau MG, Custers JH, Koudstaal W, Kostense S, Havenga MJ, et al. Immunogenicity of recombinant adenovirus serotype 35 vaccine in the presence of pre-existing anti-Ad5 immunity. J Immunol. 2004;172(10):6290-7. doi: 10.4049/jimmunol.172.10.6290. PubMed PMID: 15128818.
46. Shiver JW, Emini EA. Recent advances in the development of HIV-1 vaccines using replication-incompetent adenovirus vectors. Annu Rev Med. 2004;55:355-72. doi: 10.1146/annurev.med.55.091902.104344. PubMed PMID: 14746526.
47. Le Gars M, Sadoff J, Struyf F, Heerwegh D, Truyers C, Hendriks J, et al. Impact of Preexisting Anti-Adenovirus 26 Humoral Immunity on Immunogenicity of the Ad26.COV2.S Coronavirus Disease 2019 Vaccine. J Infect Dis. 2022;226(6):979-82. doi: 10.1093/infdis/jiac142. PubMed PMID: 35429381; PubMed Central PMCID: PMCPMC9047246.
48. Afolabi MO, Ishola D, Manno D, Keshinro B, Bockstal V, Rogers B, et al. Safety and immunogenicity of the two-dose heterologous Ad26.ZEBOV and MVA-BN-Filo Ebola vaccine regimen in children in Sierra Leone: a randomised, double-blind, controlled trial. Lancet Infect Dis. 2022;22(1):110-22. Epub 20210913. doi: 10.1016/S1473-3099(21)00128-6. PubMed PMID: 34529962; PubMed Central PMCID: PMCPMC7613317.
49. U.S. Department of Health and Human Services FaDA. Guidance for Industry. Toxicity Grading Scale for Healthy Adult and Adolescent Volunteers Enrolled in Preventive Vaccine Clinical Trials. 2007. https://www.fda.gov/media/73679/download.
50. Khoo NKH, Lim JME, Gill US, de Alwis R, Tan N, Toh JZN, et al. Differential immunogenicity of homologous versus heterologous boost in Ad26.COV2.S vaccine

recipients. Med. 2022;3(2):104-18 e4. Epub 20220119. doi: 10.1016/j.medj.2021.12.004. PubMed PMID: 35072129; PubMed Central PMCID: PMCPMC8767655.

51. Hillus D, Schwarz T, Tober-Lau P, Vanshylla K, Hastor H, Thibeault C, et al. Safety, reactogenicity, and immunogenicity of homologous and heterologous prime-boost immunisation with ChAdOx1 nCoV-19 and BNT162b2: a prospective cohort study. Lancet Respir Med. 2021;9(11):1255-65. Epub 20210813. doi: 10.1016/S2213-2600(21)00357-X. PubMed PMID: 34391547; PubMed Central PMCID: PMCPMC8360702.
52. Schmidt T, Klemis V, Schub D, Mihm J, Hielscher F, Marx S, et al. Immunogenicity and reactogenicity of heterologous ChAdOx1 nCoV-19/mRNA vaccination. Nat Med. 2021;27(9):1530-5. Epub 20210726. doi: 10.1038/s41591-021-01464-w. PubMed PMID: 34312554; PubMed Central PMCID: PMCPMC8440177.
53. Irrgang P, Gerling J, Kocher K, Lapuente D, Steininger P, Habenicht K, et al. Class switch toward noninflammatory, spike-specific IgG4 antibodies after repeated SARS-CoV-2 mRNA vaccination. Sci Immunol. 2023;8(79):eade2798. Epub 20230127. doi: 10.1126/sciimmunol.ade2798. PubMed PMID: 36548397; PubMed Central PMCID: PMCPMC9847566.
54. Buhre JS, Pongracz T, Kunsting I, Lixenfeld AS, Wang W, Nouta J, et al. mRNA vaccines against SARS-CoV-2 induce comparably low long-term IgG Fc galactosylation and sialylation levels but increasing long-term IgG4 responses compared to an adenovirus-based vaccine. Front Immunol. 2022;13:1020844. Epub 20230112. doi: 10.3389/fimmu.2022.1020844. PubMed PMID: 36713457; PubMed Central PMCID: PMCPMC9877300.
55. Brenchley JM, Price DA, Schacker TW, Asher TE, Silvestri G, Rao S, et al. Microbial translocation is a cause of systemic immune activation in chronic HIV infection. Nat Med. 2006;12(12):1365-71. Epub 20061119. doi: 10.1038/nm1511. PubMed PMID: 17115046.
56. Jedicke N, Stankov MV, Cossmann A, Dopfer-Jablonka A, Knuth C, Ahrenstorf G, et al. Humoral immune response following prime and boost BNT162b2 vaccination in people living with HIV on antiretroviral therapy. HIV Med. 2022;23(5):558-63. Epub 20211102. doi: 10.1111/hiv.13202. PubMed PMID: 34725907; PubMed Central PMCID: PMCPMC8652991.
57. Antinori A, Cicalini S, Meschi S, Bordoni V, Lorenzini P, Vergori A, et al. Humoral and Cellular Immune Response Elicited by mRNA Vaccination Against Severe Acute Respiratory Syndrome Coronavirus 2 (SARS-CoV-2) in People Living With Human Immunodeficiency Virus Receiving Antiretroviral Therapy Based on Current CD4 T-Lymphocyte Count. Clin Infect Dis. 2022;75(1):e552-e63. doi: 10.1093/cid/ciac238. PubMed PMID: 35366316; PubMed Central PMCID: PMCPMC9047161.
58. Vergori A, Cozzi Lepri A, Cicalini S, Matusali G, Bordoni V, Lanini S, et al. Immunogenicity to COVID-19 mRNA vaccine third dose in people living with HIV. Nat Commun. 2022;13(1):4922. Epub 20220822. doi: 10.1038/s41467-022-32263-7. PubMed PMID: 35995780; PubMed Central PMCID: PMCPMC9395398.

Table 1

	Arm A Full-dose Ad26.COV2.S	**Arm B** Half-dose Ad26.COV2.S	**Arm C** Full-dose BNT162b2	**Arm D** Half-dose BNT162b2	**Total**
Vaccinated (N)	74	69	73	73	289
Age*	42 (35-48)	40 (35-45)	43 (35-50)	42 (35-49)	42 (35-49)
18-29 years	5 (6.8%)	5 (7.2%)	7 (9.6%)	6 (8.2%)	23 (8%)
30-44 years	41 (55.4%)	46 (66.7%)	34 (46.6%)	34 (46.6%)	155 (53.6%)
45-54 years	20 (27%)	10 (14.5%)	23 (31.5%)	22 (30.1%)	75 (26%)
≥ 55 years	8 (10.8%)	8 (11.6%)	9 (12.3%)	11 (15.1%)	36 (12.5%)
Sex					
Male	10 (13.5%)	8 (11.6%)	18 (24.7%)	15 (20.5%)	51 (17.6%)
Female	64 (86.5%)	61 (88.4%)	55 (75.3%)	58 (79.5%)	238 (82.4%)
Ethnicity					
Black African	69 (93.2%)	67 (97.1%)	69 (94.5%)	70 (95.9%)	275 (95.2%)
Other	5 (6.8%)	2 (2.9%)	4 (5.5%)	3 (4.1%)	14 (4.8%)
Days between prime and Booster*	265 (245-292)	271 (259-302)	273 (258-291)	272 (253-300)	271 (255-296)
BMI					
Underweight	0 (0%)	2 (2.9%)	0 (0%)	1 (1.4%)	3 (1%)
Normal	12 (16.2%)	8 (11.6%)	14 (19.2%)	6 (8.2%)	40 (13.8%)
Overweight	20 (27%)	41 (59.4%)	39 (53.4%)	47 (64.4%)	71 (24.6%)
Obese	41 (55.4%)	39 (56.5%)	47 (64.4%)	47 (64.4%)	174 (60.2%)
Not available	1 (1.4%)	0 (0%)	0 (0%)	0 (0%)	0 (0%)
HIV infection					
HIV Positive	27 (36.5%)	28 (40.6%)	31 (42.5%)	30 (41.1%)	116 (40.1%)
Viremic[$] CD4 count (cells/mm^3)* Viral load (copies/mL)*	1 (3.7%) 223 (na) 818	5 (17.9%) 452 (103-471) 5838	4 (12.9%) 1136 29911	6 (20%) 341 (132-538) 19960	16 (13.8%) 452 (132-538) 15376
	na	(3054-18252)	(14863-47207)	(5324-37713)	(3054-27420)
Aviremic[$] CD4 count (cells/mm^3)*	26 (96.3%) 698 (580-923)	23 (82.1%) 677 (530-855)	27 (87.1%) 812 (623-931	24 (80%) 666 (538-737)	100 (86.2%) 708 (558-922)
Prior SARS-CoV-2 infection[&]	51/58 (87.8%)	52/57 (91.2%)	55/59 (93.2%)	55/59 (93.2%)	213/223 (91.4%)
Co-morbidities					
Hypertension	19 (25.7%)	8 (11.6%)	17 (23.3%)	17 (23.3%)	61 (21.1%)
Anaemia	7 (9.5%)	8 (11.6%)	6 (8.2%)	9 (12.3%)	30 (10.4%)
Asthma	6 (8.1%)	3 (4.3%)	2 (2.7%)	1 (1.4%)	12 (4.2%)
Diabetes mellitus	3 (4.1%)	1 (1.4%)	4 (5.5%)	4 (5.5%)	12 (4.2%)
Arthritis	1 (1.4%)	0 (0%)	3 (4.1%)	3 (4.1%)	7 (2.4%)
Tuberculosis	0 (0%)	4 (5.8%)	2 (2.7%)	0 (0%)	6 (2.1%)
Retention					
W2 visits completed	74 (100%)	66 (95.7%)	72 (98.6%)	69 (94.5%)	281 (97.2%)
W12 visits completed	74 (100%)	67 (97.1%)	67 (91.8%)	70 (95.9%)	278 (96.2%)
W24 visits completed	69 (93.2%)	63 (91.3%)	69 (94.5%)	68 (93.2%)	269 (93.1%)

Table 1: Clinical Characteristics of study participants
Unless specified, all data are presented as n (%N); *median and interquartile range (IQR); [$]% is of all HIV-infected participants; Viremic individuals were defined as having a HIV-1 viral load (VL) >200 HIV mRNA copies/mm^3; 3 participants in the viremic arm C had a missing CD4 count; [&]Prior SARS-CoV-2 infection was defined by the presence of Nucleocapsid-specific IgG; na: non-applicable.

Figure 1

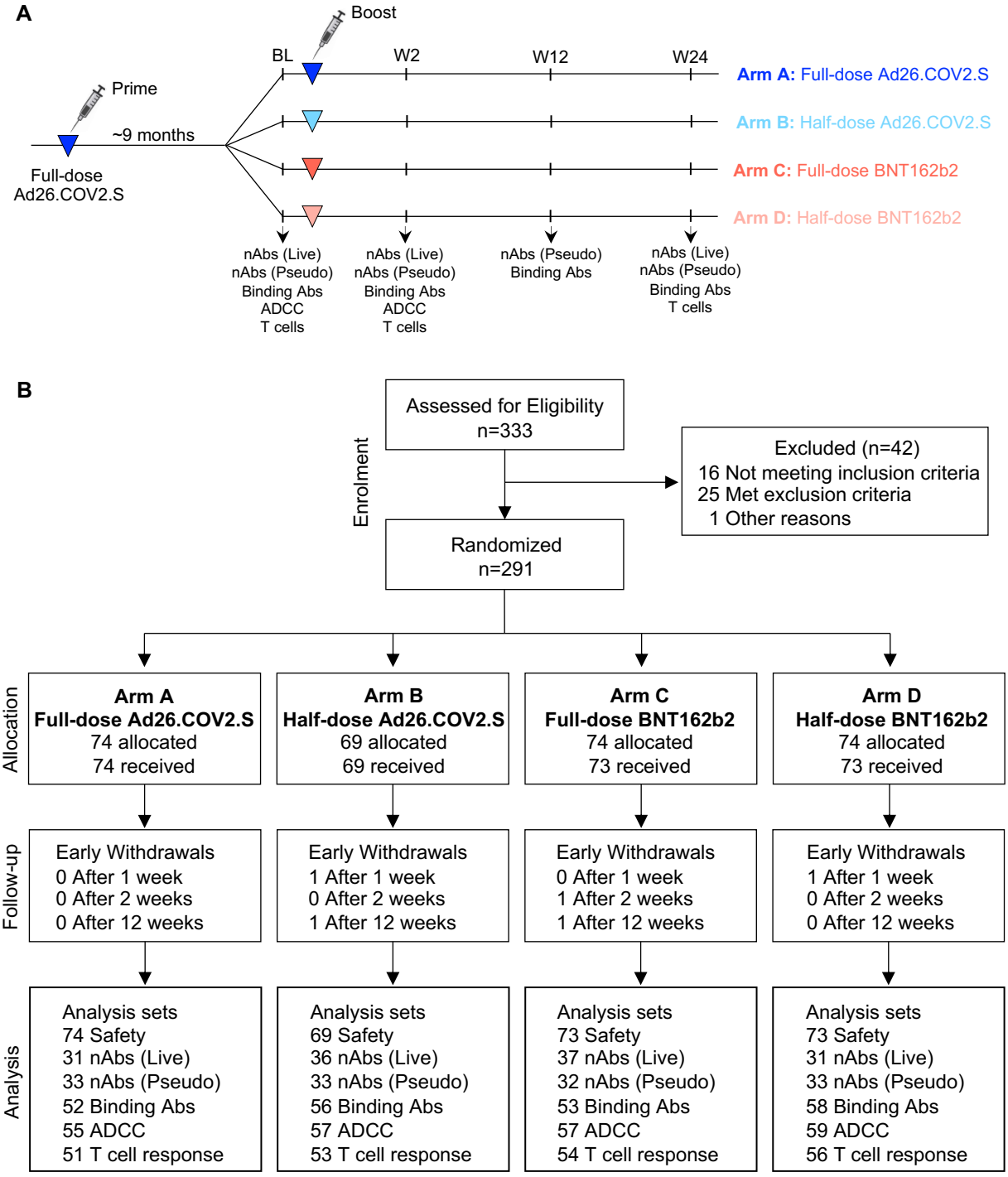
A
Boost
BL
W2
W12
W24
Prime
~9 months
Full-dose
Ad26.COV2.S
Arm A: Full-dose Ad26.COV2.S
Arm B: Half-dose Ad26.COV2.S
Arm C: Full-dose BNT162b2
Arm D: Half-dose BNT162b2
nAbs (Live)
nAbs (Pseudo)
Binding Abs
ADCC
T cells
nAbs (Live)
nAbs (Pseudo)
Binding Abs
ADCC
T cells
nAbs (Pseudo)
Binding Abs
nAbs (Live)
nAbs (Pseudo)
Binding Abs
T cells
B
Enrolment
Assessed for Eligibility
n=333
Excluded (n=42)
16 Not meeting inclusion criteria
25 Met exclusion criteria
1 Other reasons
Randomized
n=291
Allocation
Arm A
Full-dose Ad26.COV2.S
74 allocated
74 received
Arm B
Half-dose Ad26.COV2.S
69 allocated
69 received
Arm C
Full-dose BNT162b2
74 allocated
73 received
Arm D
Half-dose BNT162b2
74 allocated
73 received
Follow-up
Early Withdrawals
0 After 1 week
0 After 2 weeks
0 After 12 weeks
Early Withdrawals
1 After 1 week
0 After 2 weeks
1 After 12 weeks
Early Withdrawals
0 After 1 week
1 After 2 weeks
1 After 12 weeks
Early Withdrawals
1 After 1 week
0 After 2 weeks
0 After 12 weeks
Analysis
Analysis sets
74 Safety
31 nAbs (Live)
33 nAbs (Pseudo)
52 Binding Abs
55 ADCC
51 T cell response
Analysis sets
69 Safety
36 nAbs (Live)
33 nAbs (Pseudo)
56 Binding Abs
57 ADCC
53 T cell response
Analysis sets
73 Safety
37 nAbs (Live)
32 nAbs (Pseudo)
53 Binding Abs
57 ADCC
54 T cell response
Analysis sets
73 Safety
31 nAbs (Live)
33 nAbs (Pseudo)
58 Binding Abs
59 ADCC
56 T cell response

Figure 2

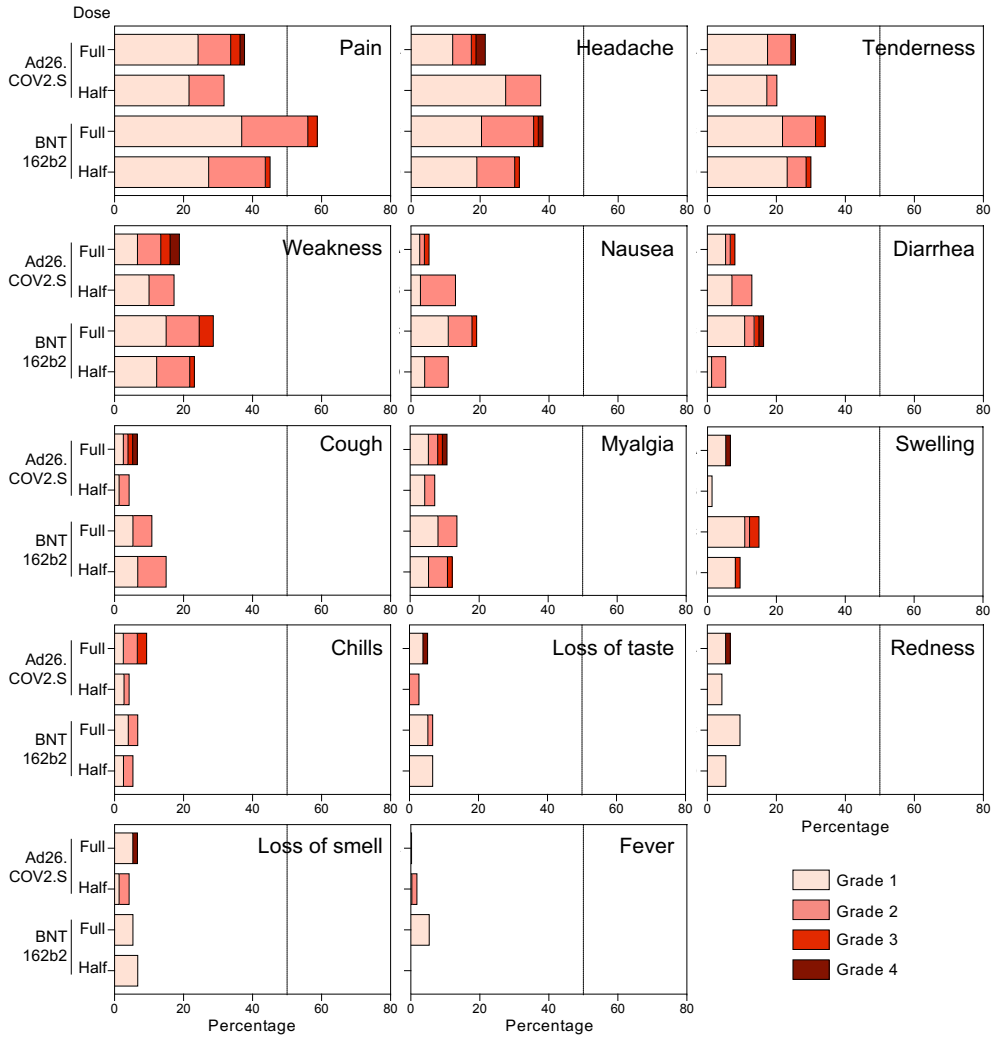
Dose
Ad26.
COV2.S
BNT
162b2
Full
Half
Pain
Headache
Tenderness
Weakness
Nausea
Diarrhea
Cough
Myalgia
Swelling
Chills
Loss of taste
Redness
Loss of smell
Fever
0
20
40
60
80
Percentage
Grade 1
Grade 2
Grade 3
Grade 4

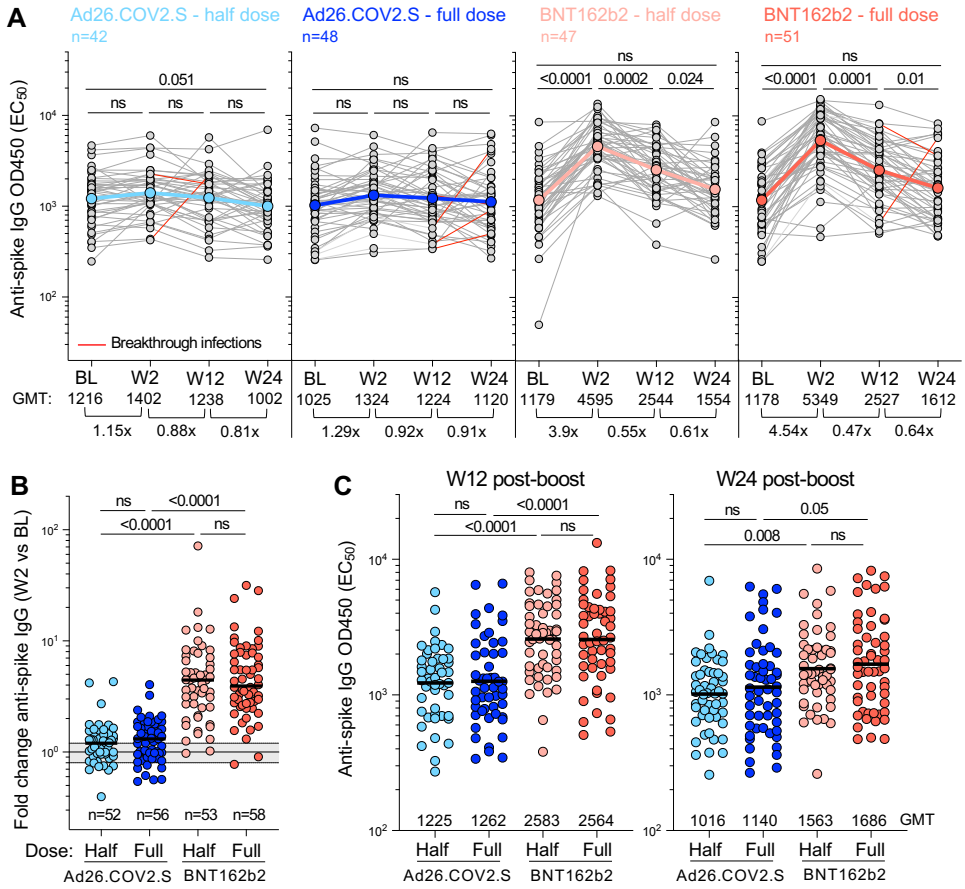
A
Ad26.COV2.S - half dose
n=42
Ad26.COV2.S - full dose
n=48
BNT162b2 - half dose
n=47
BNT162b2 - full dose
n=51
Anti-spike IgG OD450 (EC50)
0.051
ns
<0.0001
0.0002
0.024
0.0001
0.01
Breakthrough infections
BL W2 W12 W24
GMT: 1216 1402 1238 1002
1.15x 0.88x 0.81x
1025 1324 1224 1120
1.29x 0.92x 0.91x
1179 4595 2544 1554
3.9x 0.55x 0.61x
1178 5349 2527 1612
4.54x 0.47x 0.64x
B
Fold change anti-spike IgG (W2 vs BL)
<0.0001
n=52 n=56 n=53 n=58
Dose: Half Full Half Full
Ad26.COV2.S BNT162b2
C
W12 post-boost
W24 post-boost
0.05
0.008
1225 1262 2583 2564
1016 1140 1563 1686 GMT

Figure 4

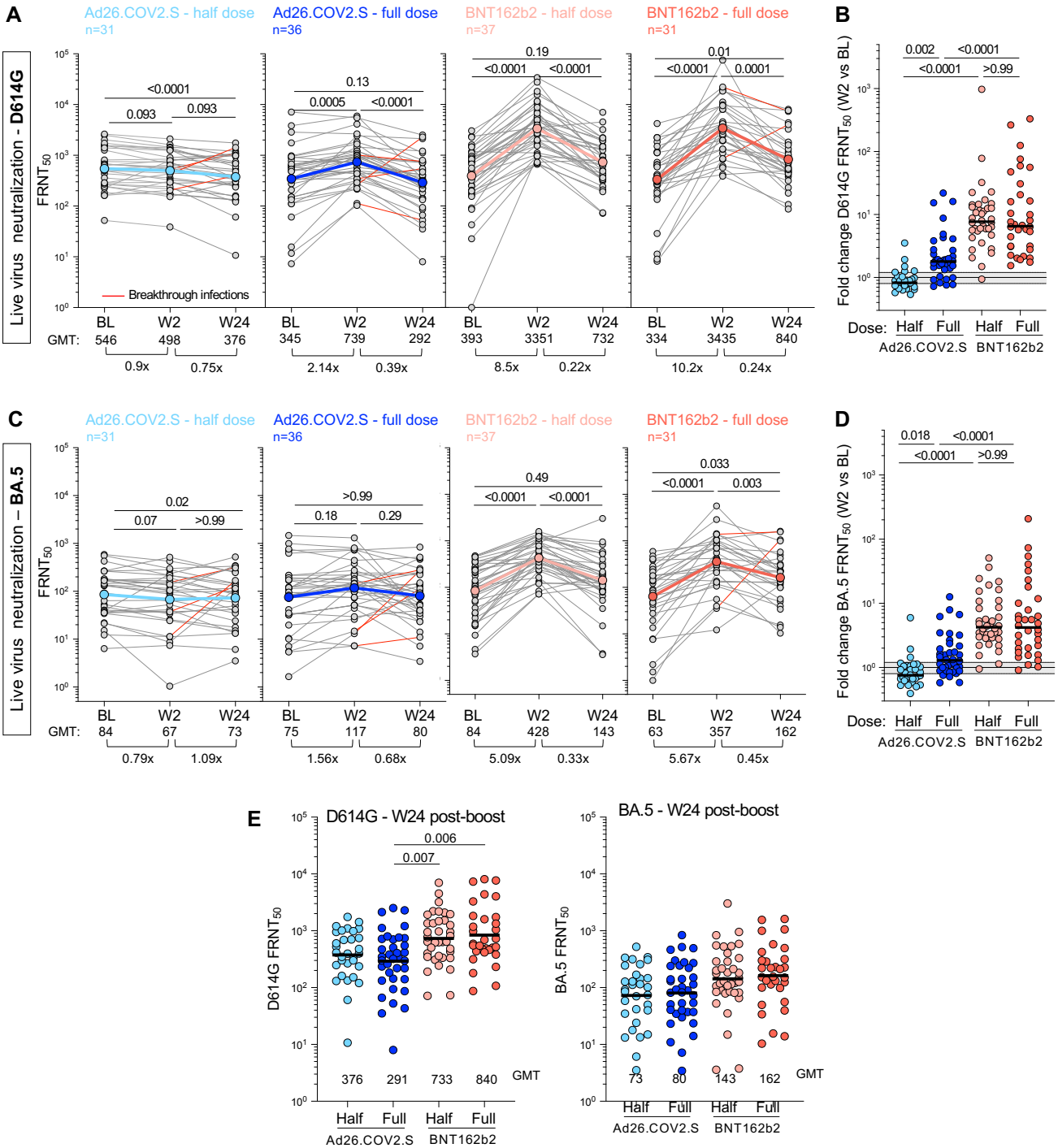
A
Ad26.COV2.S - half dose
n=31
Ad26.COV2.S - full dose
n=36
BNT162b2 - half dose
n=37
BNT162b2 - full dose
n=31
Live virus neutralization - D614G
FRNT50
Breakthrough infections
BL W2 W24
GMT: 546 498 376
0.9x 0.75x
GMT: 345 739 292
2.14x 0.39x
GMT: 393 3351 732
8.5x 0.22x
GMT: 334 3435 840
10.2x 0.24x
B
Fold change D614G FRNT50 (W2 vs BL)
Dose: Half Full Half Full
Ad26.COV2.S BNT162b2
C
Live virus neutralization – BA.5
GMT: 84 67 73
0.79x 1.09x
GMT: 75 117 80
1.56x 0.68x
GMT: 84 428 143
5.09x 0.33x
GMT: 63 357 162
5.67x 0.45x
D
Fold change BA.5 FRNT50 (W2 vs BL)
E
D614G - W24 post-boost
BA.5 - W24 post-boost
376 291 733 840 GMT
73 80 143 162 GMT

Figure 5

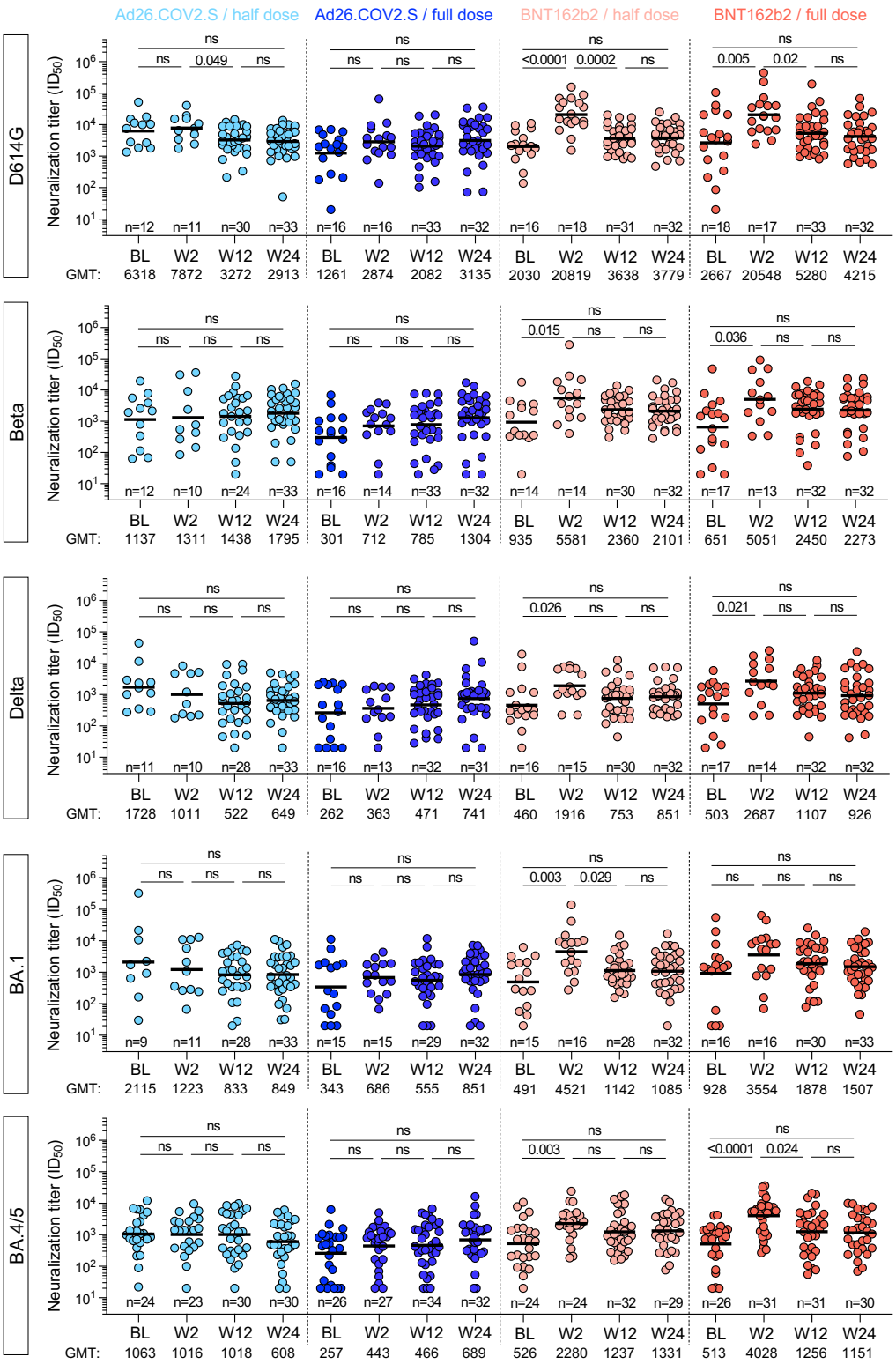
Ad26.COV2.S / half dose
Ad26.COV2.S / full dose
BNT162b2 / half dose
BNT162b2 / full dose
D614G
Beta
Delta
BA.1
BA.4/5
Neuralization titer (ID50)
BL W2 W12 W24
GMT:
D614G: ns ns 0.049 ns | ns ns ns ns | ns <0.0001 0.0002 ns | ns 0.005 0.02 ns
n=12 n=11 n=30 n=33 | n=16 n=16 n=33 n=32 | n=16 n=18 n=31 n=32 | n=18 n=17 n=33 n=32
GMT: 6318 7872 3272 2913 | 1261 2874 2082 3135 | 2030 20819 3638 3779 | 2667 20548 5280 4215
Beta: ns ns ns ns | ns ns ns ns | ns 0.015 ns ns | ns 0.036 ns ns
n=12 n=10 n=24 n=33 | n=16 n=14 n=33 n=32 | n=14 n=14 n=30 n=32 | n=17 n=13 n=32 n=32
GMT: 1137 1311 1438 1795 | 301 712 785 1304 | 935 5581 2360 2101 | 651 5051 2450 2273
Delta: ns ns ns ns | ns ns ns ns | ns 0.026 ns ns | ns 0.021 ns ns
n=11 n=10 n=28 n=33 | n=16 n=13 n=32 n=31 | n=16 n=15 n=30 n=32 | n=17 n=14 n=32 n=32
GMT: 1728 1011 522 649 | 262 363 471 741 | 460 1916 753 851 | 503 2687 1107 926
BA.1: ns ns ns ns | ns ns ns ns | ns 0.003 0.029 ns | ns ns ns ns
n=9 n=11 n=28 n=33 | n=15 n=15 n=29 n=32 | n=15 n=16 n=28 n=32 | n=16 n=16 n=30 n=33
GMT: 2115 1223 833 849 | 343 686 555 851 | 491 4521 1142 1085 | 928 3554 1878 1507
BA.4/5: ns ns ns ns | ns ns ns ns | ns 0.003 ns ns | ns <0.0001 0.024 ns
n=24 n=23 n=30 n=30 | n=26 n=27 n=34 n=32 | n=24 n=24 n=32 n=29 | n=26 n=31 n=31 n=30
GMT: 1063 1016 1018 608 | 257 443 466 689 | 526 2280 1237 1331 | 513 4028 1256 1151

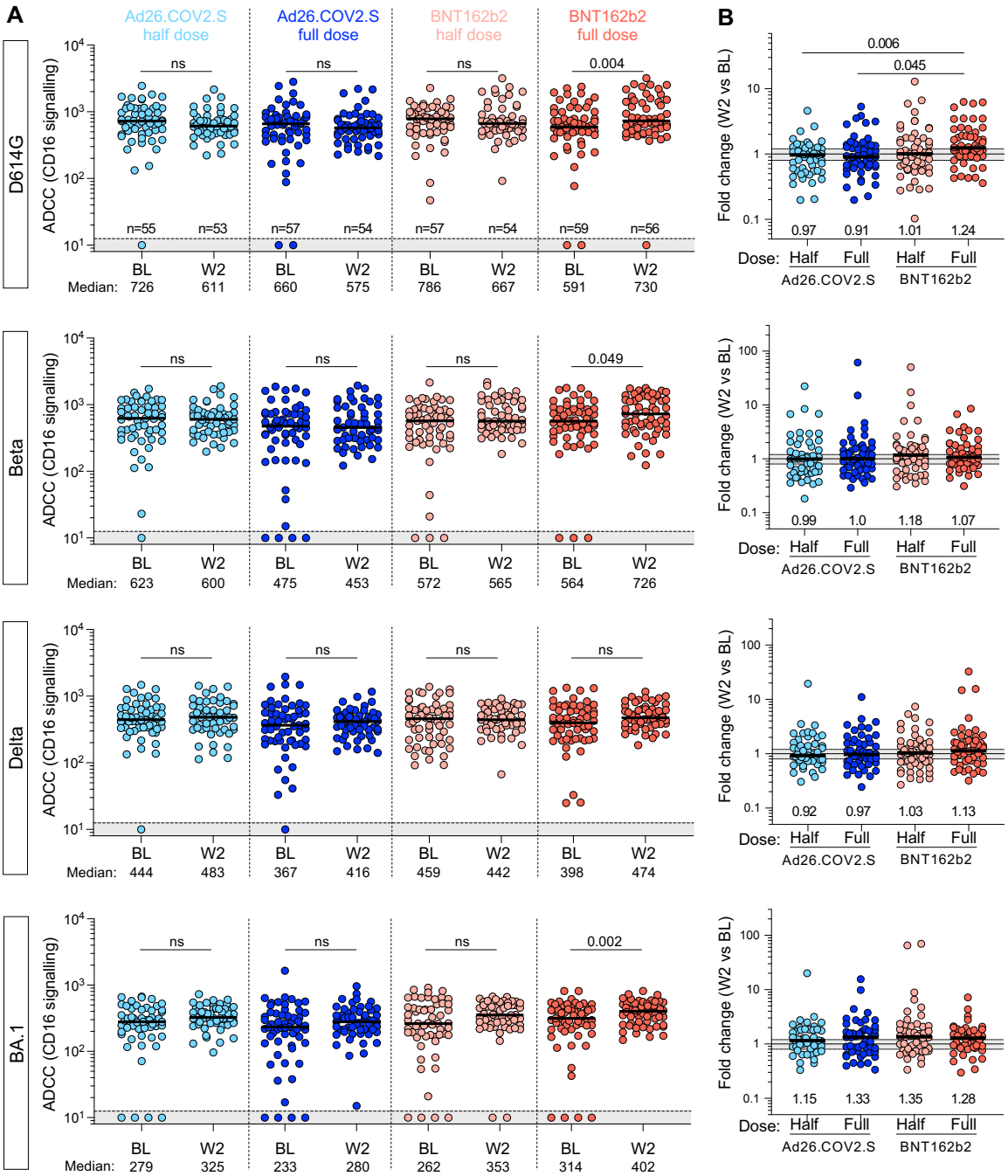
A
B
Ad26.COV2.S half dose
Ad26.COV2.S full dose
BNT162b2 half dose
BNT162b2 full dose
D614G
Beta
Delta
BA.1
ADCC (CD16 signalling)
Fold change (W2 vs BL)
ns
0.004
0.049
0.002
0.006
0.045
n=55
n=53
n=57
n=54
n=57
n=54
n=59
n=56
BL
W2
Median: 726 611 660 575 786 667 591 730
Median: 623 600 475 453 572 565 564 726
Median: 444 483 367 416 459 442 398 474
Median: 279 325 233 280 262 353 314 402
0.97 0.91 1.01 1.24
0.99 1.0 1.18 1.07
0.92 0.97 1.03 1.13
1.15 1.33 1.35 1.28
Dose: Half Full Half Full
Ad26.COV2.S
BNT162b2

Figure 7

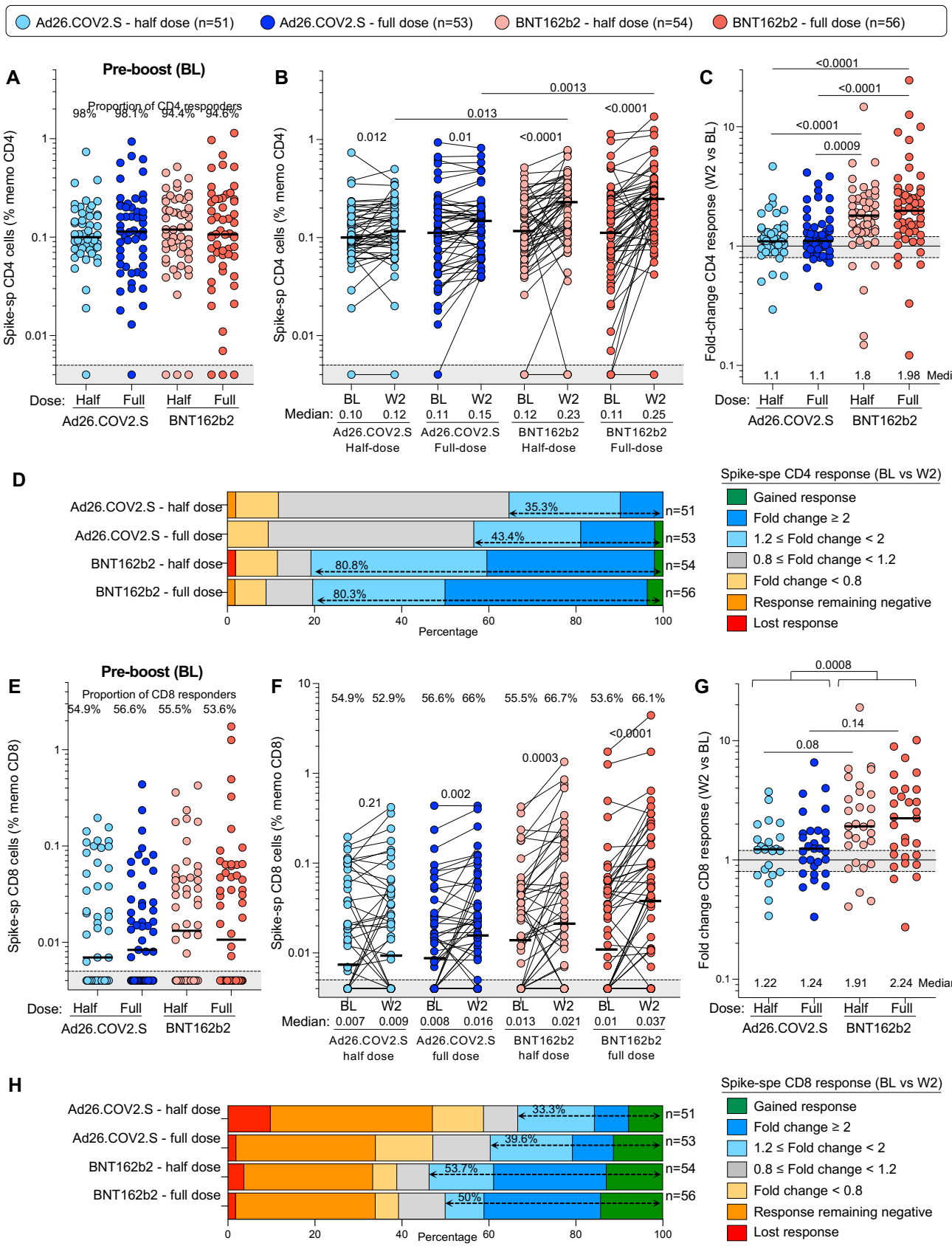
Ad26.COV2.S - half dose (n=51)
Ad26.COV2.S - full dose (n=53)
BNT162b2 - half dose (n=54)
BNT162b2 - full dose (n=56)
A
Pre-boost (BL)
Proportion of CD4 responders
98% 98.1% 94.4% 94.6%
Spike-sp CD4 cells (% memo CD4)
Dose: Half Full Half Full
Ad26.COV2.S BNT162b2
B
0.012 0.01 <0.0001 <0.0001
0.013 0.0013
Median: 0.10 0.12 0.11 0.15 0.12 0.23 0.11 0.25
Ad26.COV2.S Half-dose
Ad26.COV2.S Full-dose
BNT162b2 Half-dose
BNT162b2 Full-dose
C
<0.0001 <0.0001 <0.0001 0.0009
Fold-change CD4 response (W2 vs BL)
1.1 1.1 1.8 1.98 Median
D
Ad26.COV2.S - half dose
Ad26.COV2.S - full dose
BNT162b2 - half dose
BNT162b2 - full dose
35.3% 43.4% 80.8% 80.3%
n=51 n=53 n=54 n=56
Percentage
Spike-spe CD4 response (BL vs W2)
Gained response
Fold change ≥ 2
1.2 ≤ Fold change < 2
0.8 ≤ Fold change < 1.2
Fold change < 0.8
Response remaining negative
Lost response
E
Pre-boost (BL)
Proportion of CD8 responders
54.9% 56.6% 55.5% 53.6%
Spike-sp CD8 cells (% memo CD8)
F
54.9% 52.9% 56.6% 66% 55.5% 66.7% 53.6% 66.1%
0.21 0.002 0.0003 <0.0001
Median: 0.007 0.009 0.008 0.016 0.013 0.021 0.01 0.037
G
0.0008 0.14 0.08
Fold change CD8 response (W2 vs BL)
1.22 1.24 1.91 2.24 Median
H
33.3% 39.6% 53.7% 50%
Spike-spe CD8 response (BL vs W2)

Figure 8

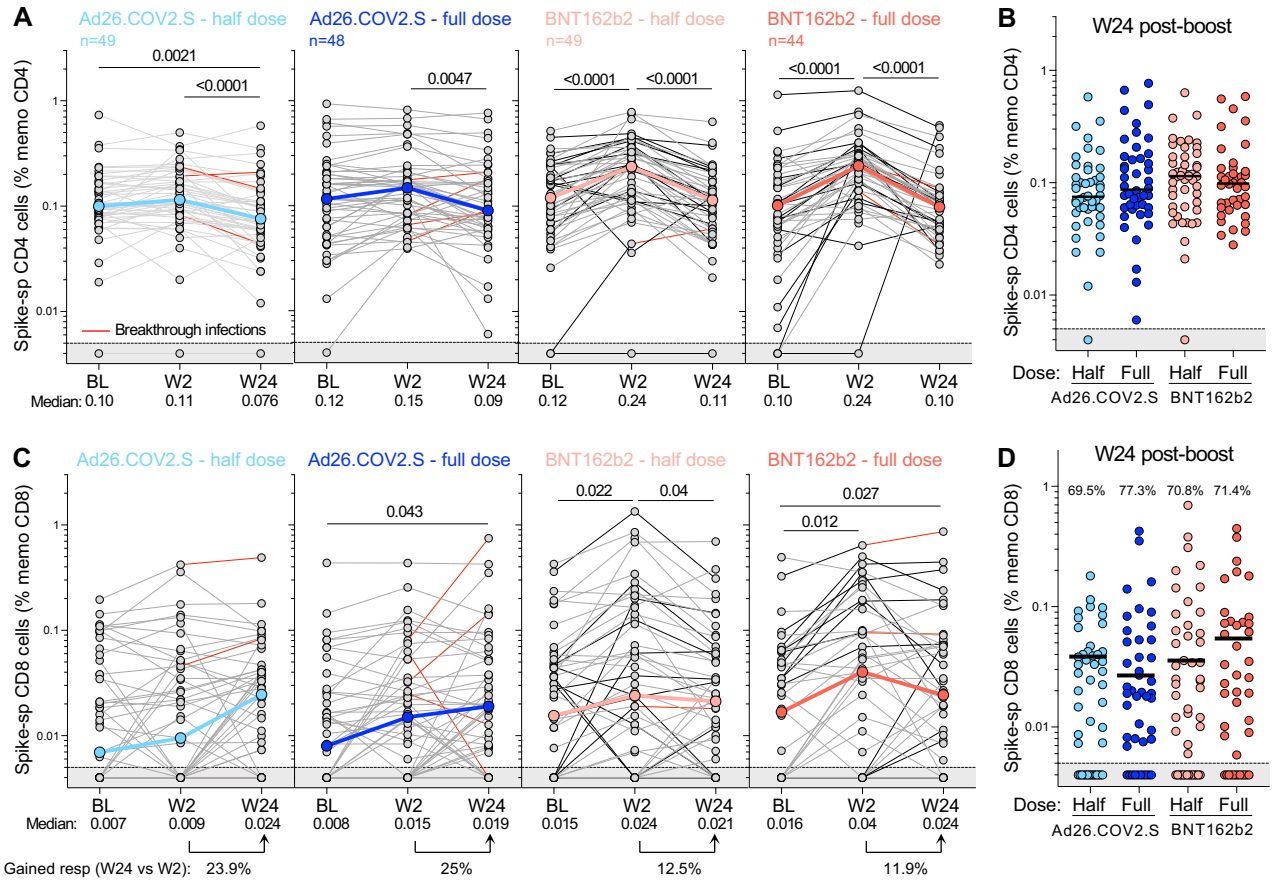
A
Ad26.COV2.S - half dose
n=49
Ad26.COV2.S - full dose
n=48
BNT162b2 - half dose
n=49
BNT162b2 - full dose
n=44
Spike-sp CD4 cells (% memo CD4)
0.0021
<0.0001
0.0047
<0.0001
<0.0001
<0.0001
<0.0001
Breakthrough infections
BL W2 W24
Median: 0.10 0.11 0.076
0.12 0.15 0.09
0.12 0.24 0.11
0.10 0.24 0.10
B
W24 post-boost
Spike-sp CD4 cells (% memo CD4)
Dose: Half Full Half Full
Ad26.COV2.S BNT162b2
C
Ad26.COV2.S - half dose
Ad26.COV2.S - full dose
BNT162b2 - half dose
BNT162b2 - full dose
Spike-sp CD8 cells (% memo CD8)
0.043
0.022
0.04
0.027
0.012
Median: 0.007 0.009 0.024
0.008 0.015 0.019
0.015 0.024 0.021
0.016 0.04 0.024
Gained resp (W24 vs W2): 23.9% 25% 12.5% 11.9%
D
W24 post-boost
69.5% 77.3% 70.8% 71.4%
Spike-sp CD8 cells (% memo CD8)
Dose: Half Full Half Full
Ad26.COV2.S BNT162b2

Figure 9

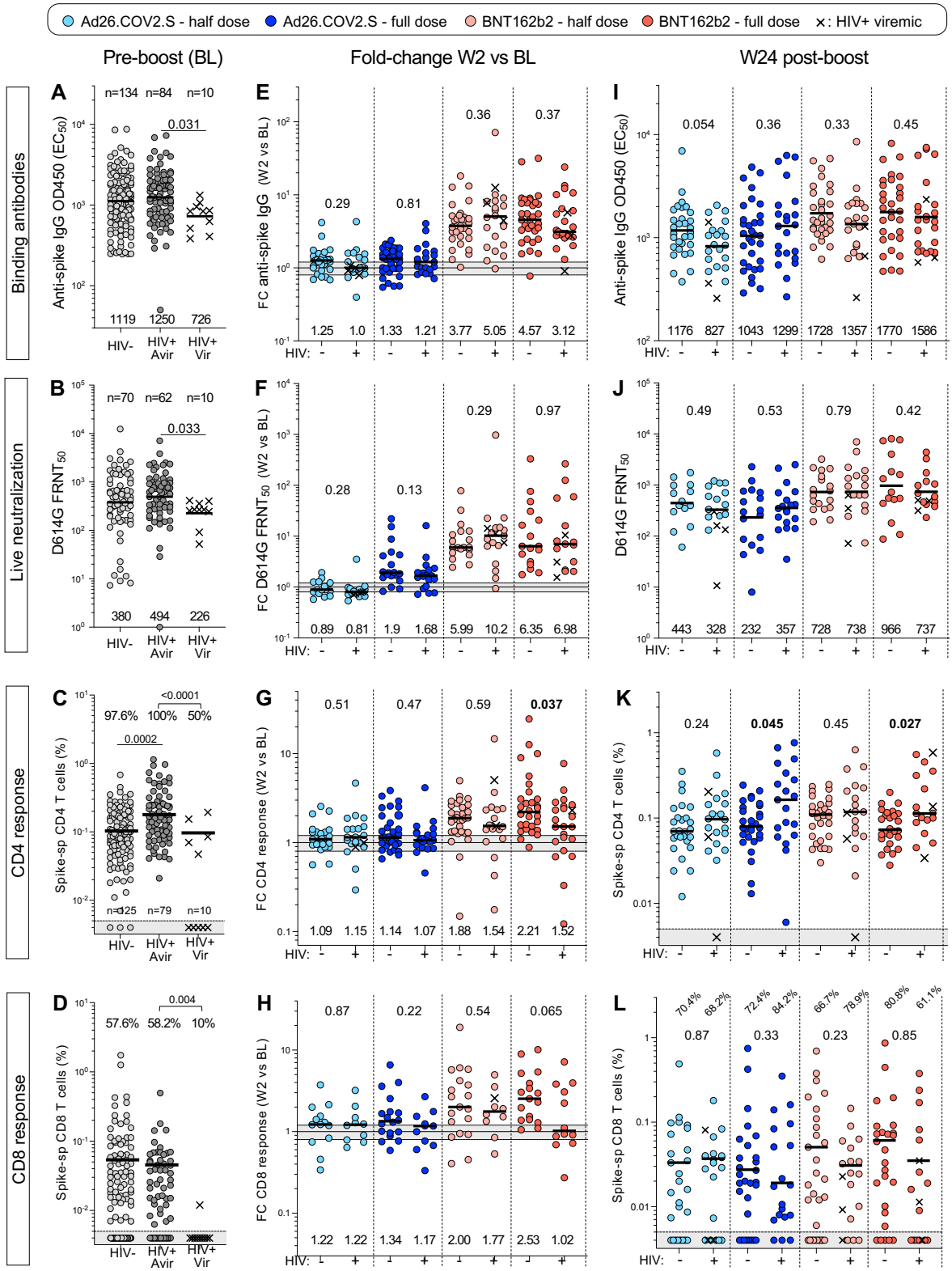
Ad26.COV2.S - half dose
Ad26.COV2.S - full dose
BNT162b2 - half dose
BNT162b2 - full dose
×: HIV+ viremic
Pre-boost (BL)
Fold-change W2 vs BL
W24 post-boost
Binding antibodies
Live neutralization
CD4 response
CD8 response
A
B
C
D
E
F
G
H
I
J
K
L
Anti-spike IgG OD450 (EC50)
D614G FRNT50
Spike-sp CD4 T cells (%)
Spike-sp CD8 T cells (%)
FC anti-spike IgG (W2 vs BL)
FC D614G FRNT50 (W2 vs BL)
FC CD4 response (W2 vs BL)
FC CD8 response (W2 vs BL)
HIV-
HIV+ Avir
HIV+ Vir
HIV:

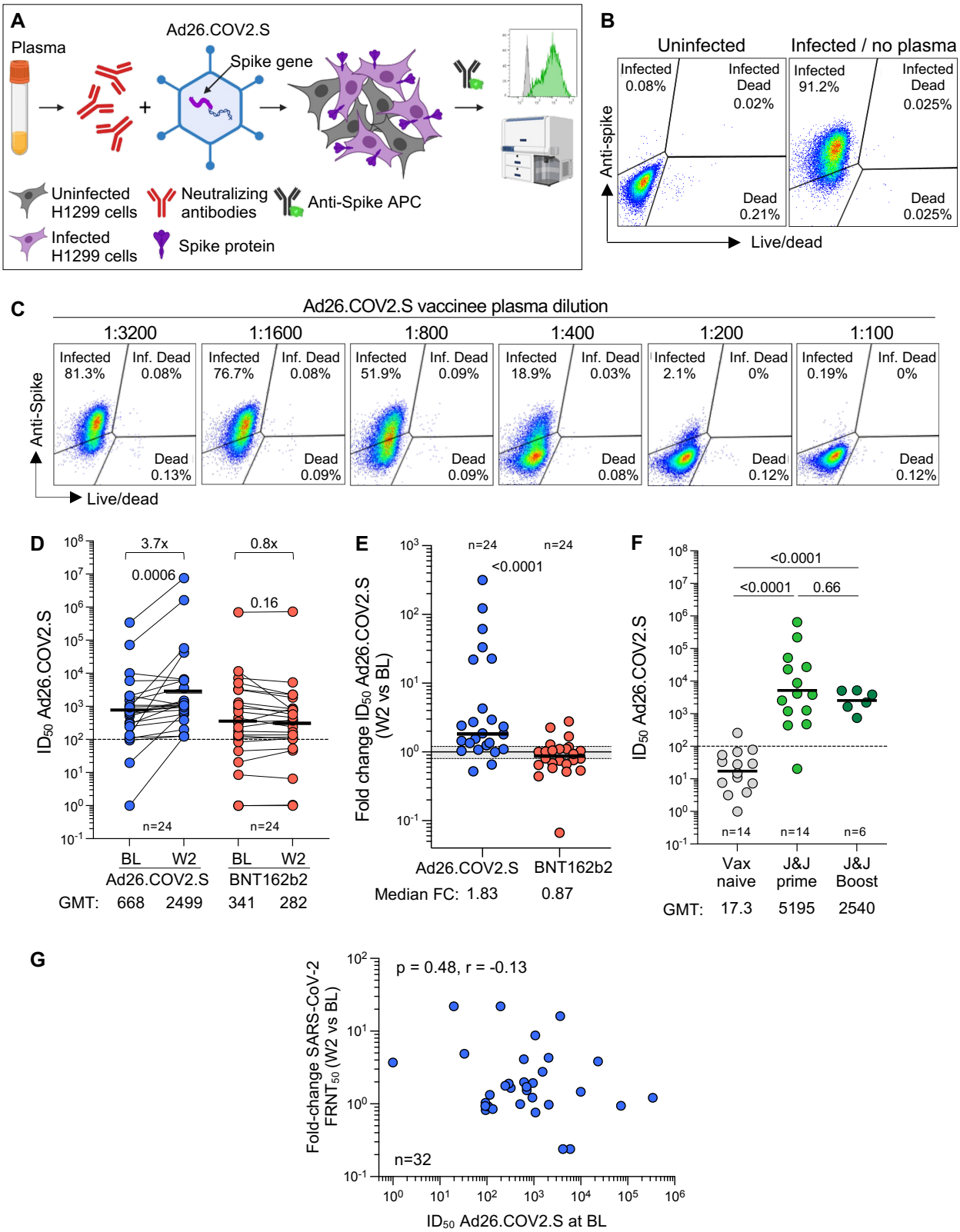
A
Plasma
Ad26.COV2.S
Spike gene
Uninfected H1299 cells
Neutralizing antibodies
Anti-Spike APC
Infected H1299 cells
Spike protein
B
Uninfected
Infected / no plasma
Infected 0.08%
Infected Dead 0.02%
Dead 0.21%
Infected 91.2%
Infected Dead 0.025%
Dead 0.025%
Anti-spike
Live/dead
C
Ad26.COV2.S vaccinee plasma dilution
1:3200
1:1600
1:800
1:400
1:200
1:100
Infected 81.3%
Inf. Dead 0.08%
Dead 0.13%
Infected 76.7%
Inf. Dead 0.08%
Dead 0.09%
Infected 51.9%
Inf. Dead 0.09%
Dead 0.09%
Infected 18.9%
Inf. Dead 0.03%
Dead 0.08%
Infected 2.1%
Inf. Dead 0%
Dead 0.12%
Infected 0.19%
Inf. Dead 0%
Dead 0.12%
Anti-Spike
Live/dead
D
3.7x
0.8x
0.0006
0.16
n=24
n=24
ID50 Ad26.COV2.S
BL W2 BL W2
Ad26.COV2.S BNT162b2
GMT: 668 2499 341 282
E
n=24 n=24
<0.0001
Fold change ID50 Ad26.COV2.S (W2 vs BL)
Ad26.COV2.S BNT162b2
Median FC: 1.83 0.87
F
<0.0001
<0.0001 0.66
ID50 Ad26.COV2.S
n=14 n=14 n=6
Vax naive J&J prime J&J Boost
GMT: 17.3 5195 2540
G
p = 0.48, r = -0.13
n=32
Fold-change SARS-CoV-2 FRNT50 (W2 vs BL)
ID50 Ad26.COV2.S at BL

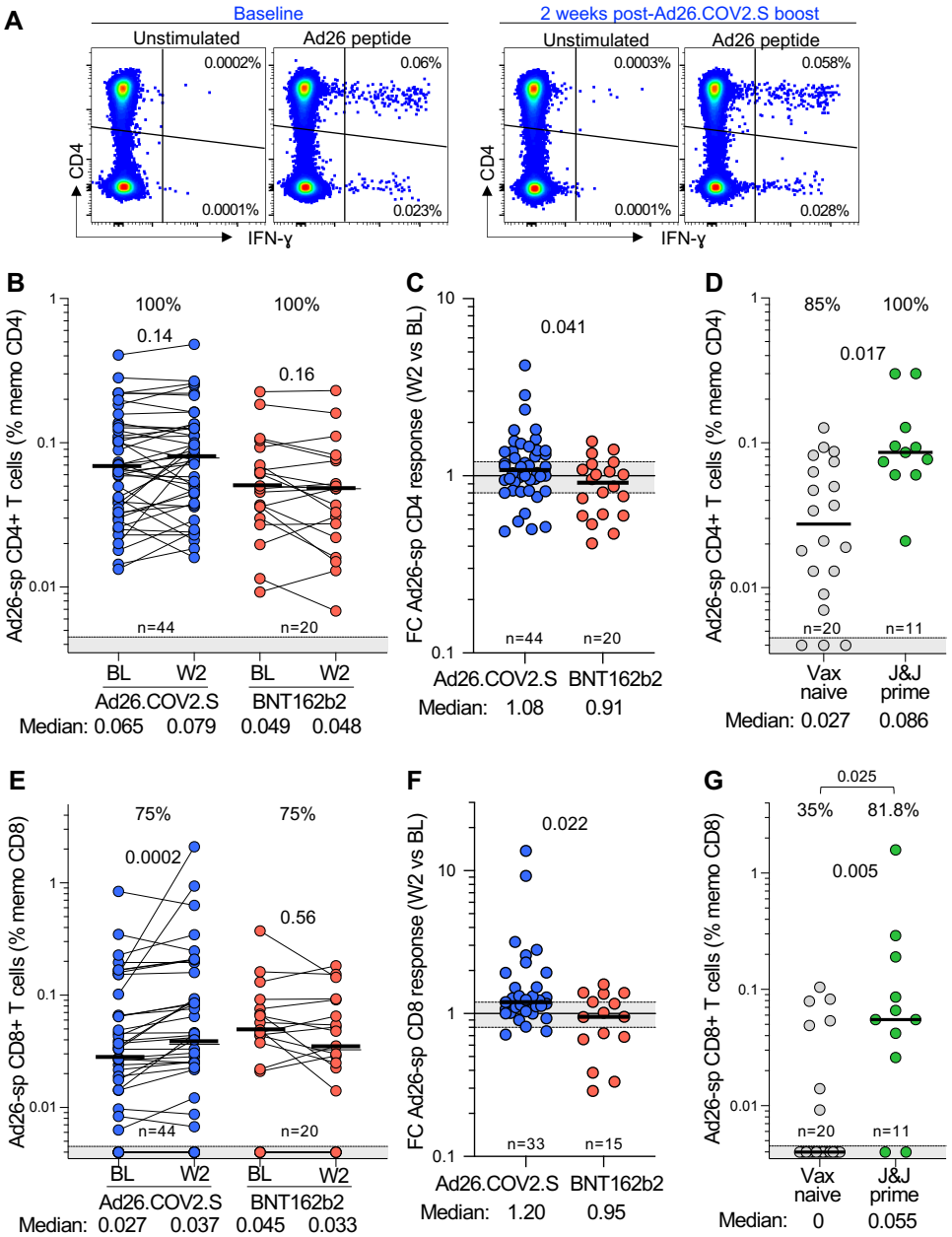

H

	Spike-sp CD4 T cell (%)		Spike-sp CD8 T cell (%)		FC Spike CD4
	BL	W2	BL	W2	W2 vs BL
Ad26-sp CD4 T cells (%) at BL	p = 0.11 r = 0.24	p = 0.25 r = 0.18	p = 0.05 r = 0.30	p = 0.16 r = 0.29	p = 0.08 r = -0.27
Ad26-sp CD8 T cells (%) at BL	p = 0.001 r = 0.47	p = 0.016 r = 0.37	p = 0.007 r = 0.40	p = 0.009 r = 0.39	p = 0.037 r = -0.32

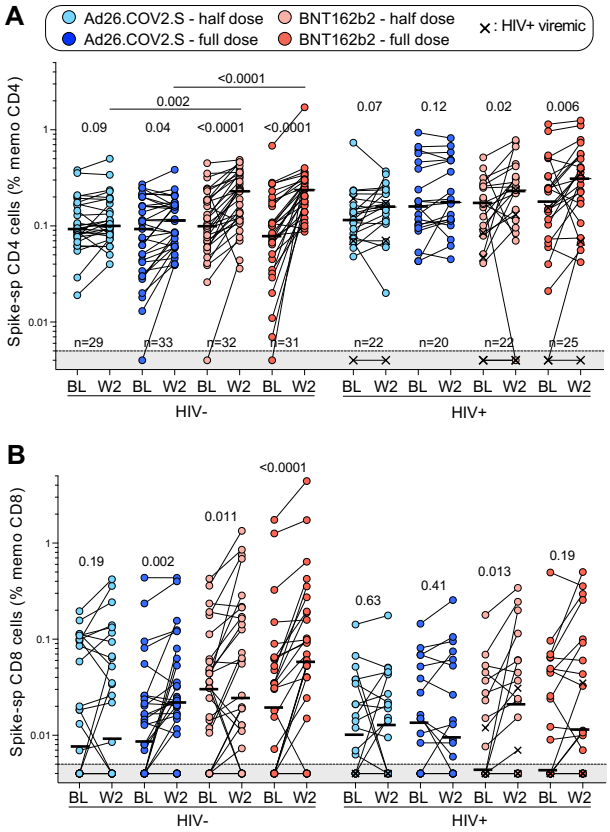

Supplemental Figure 1: SARS-CoV-2 spike-specific T cell responses in participants stratified by HIV status in each study arm. Frequency of spike-specific CD4+ T cells **(A)** and spike-specific CD8+ T cells **(B)** before (BL) and 2 weeks after vaccine boost (W2) in HIV-negative participants and in PLWH. Bars represent medians. Viremic PLWH are identified with a cross. Bars represent medians. A two-tailed Wilcoxon signed-rank test was used to assess statistical differences between paired samples and a Kruskal-Wallis with Dunn's corrections was used to compare different groups.

Supp Table 1

	Vax-naive	J&J primed	J&J boosted
N	14	14	6
Age*	46 (37-57)	46 (37-57)	55 (49-57)
Gender (% female)	100%	100%	100%
Time since last vaccination (days)*	na	44 (31-53)	110 (96-117)

Supplementary Table 1: Clinical characteristics of samples used for Ad26-specific antibody response assessment. (Related to Figure 10F). *: Median and Interquartile range (IQR), na: not applicable.

Supp Table 2

	Vax-naive	J&J primed
N	20	11
Age*	43 (33-53)	49 (32-53)
Gender (% female)	90%	81.8%
Time since vaccination (days)*	na	25 (20-45)

Supplementary Table 2: Clinical characteristics of samples used for Ad26-specific T cell response assessment. (Related to Figures 11D and 11G). All participants were HIV-uninfected. *: Median and Interquartile range (IQR). na: not applicable.